JCI The Journal of Clinical Investigation

The TGR5 receptor mediates bile acid–induced itch and analgesia

Farzad Alemi, … , Nigel W. Bunnett, Carlos U. Corvera

J Clin Invest. 2013;123(4):1513-1530. https://doi.org/10.1172/JCI64551.

Research Article **Hepatology**

Patients with cholestatic disease exhibit pruritus and analgesia, but the mechanisms underlying these symptoms are unknown. We report that bile acids, which are elevated in the circulation and tissues during cholestasis, cause itch and analgesia by activating the GPCR TGR5. TGR5 was detected in peptidergic neurons of mouse dorsal root ganglia and spinal cord that transmit itch and pain, and in dermal macrophages that contain opioids. Bile acids and a TGR5-selective agonist induced hyperexcitability of dorsal root ganglia neurons and stimulated the release of the itch and analgesia transmitters gastrin-releasing peptide and leucine-enkephalin. Intradermal injection of bile acids and a TGR5-selective agonist stimulated scratching behavior by gastrin-releasing peptide– and opioid-dependent mechanisms in mice. Scratching was attenuated in *Tgr5*-KO mice but exacerbated in *Tgr5*-Tg mice (overexpressing mouse TGR5), which exhibited spontaneous pruritus. Intraplantar and intrathecal injection of bile acids caused analgesia to mechanical stimulation of the paw by an opioid-dependent mechanism. Both peripheral and central mechanisms of analgesia were absent from *Tgr5*-KO mice. Thus, bile acids activate TGR5 on sensory nerves, stimulating the release of neuropeptides in the spinal cord that transmit itch and analgesia. These mechanisms could contribute to pruritus and painless jaundice that occur during cholestatic liver diseases.

The TGR5 receptor mediates bile acid–induced itch and analgesia

Farzad Alemi,[1] Edwin Kwon,[1] Daniel P. Poole,[2] TinaMarie Lieu,[3] Victoria Lyo,[1] Fiore Cattaruzza,[1] Ferda Cevikbas,[4] Martin Steinhoff,[4] Romina Nassini,[5] Serena Materazzi,[5] Raquel Guerrero-Alba,[6] Eduardo Valdez-Morales,[6] Graeme S. Cottrell,[7] Kristina Schoonjans,[8] Pierangelo Geppetti,[5] Stephen J. Vanner,[6] Nigel W. Bunnett,[3] and Carlos U. Corvera[1]

[1]Department of Surgery, UCSF, San Francisco, California, USA. [2]Department of Anatomy and Neuroscience, University of Melbourne, Parkville, Victoria, Australia. [3]Monash Institute of Pharmaceutical Sciences, Parkville, Victoria, Australia. [4]Department of Dermatology, UCSF, San Francisco, California, USA. [5]Department of Preclinical and Clinical Pharmacology, University of Florence, Florence, Italy. [6]Gastrointestinal Diseases Research Unit, Division of Gastroenterology, Queen's University, Kingston, Ontario, Canada. [7]Department of Pharmacy and Pharmacology, The University of Bath, Bath, United Kingdom. [8]Laboratory of Integrative and Systems Physiology, Institute of Bioengineering, School of Life Sciences, Lausanne, Switzerland.

Patients with cholestatic disease exhibit pruritus and analgesia, but the mechanisms underlying these symptoms are unknown. We report that bile acids, which are elevated in the circulation and tissues during cholestasis, cause itch and analgesia by activating the GPCR TGR5. TGR5 was detected in peptidergic neurons of mouse dorsal root ganglia and spinal cord that transmit itch and pain, and in dermal macrophages that contain opioids. Bile acids and a TGR5-selective agonist induced hyperexcitability of dorsal root ganglia neurons and stimulated the release of the itch and analgesia transmitters gastrin-releasing peptide and leucine-enkephalin. Intradermal injection of bile acids and a TGR5-selective agonist stimulated scratching behavior by gastrin-releasing peptide– and opioid-dependent mechanisms in mice. Scratching was attenuated in *Tgr5*-KO mice but exacerbated in *Tgr5*-Tg mice (overexpressing mouse TGR5), which exhibited spontaneous pruritus. Intraplantar and intrathecal injection of bile acids caused analgesia to mechanical stimulation of the paw by an opioid-dependent mechanism. Both peripheral and central mechanisms of analgesia were absent from *Tgr5*-KO mice. Thus, bile acids activate TGR5 on sensory nerves, stimulating the release of neuropeptides in the spinal cord that transmit itch and analgesia. These mechanisms could contribute to pruritus and painless jaundice that occur during cholestatic liver diseases.

Introduction

Patients with cholestatic liver diseases, characterized by diminished delivery of bile into the intestine, can experience severe and intractable pruritus that is an indication for liver transplantation (1, 2). Cholestatic patients can also exhibit altered pain perception. Jaundice in the absence of abdominal pain ("painless jaundice") suggests gradual malignant obstruction of the biliary tract, whereas painful jaundice (cholangitis) is associated with an acute obstruction with gallstones, as recognized by Courvoisier a century ago (3). Patients undergoing orthotopic liver transplantation for cholestatic diseases report lower postoperative pain scores and require less morphine analgesia than patients undergoing liver resection, despite the more extensive transplantation procedure (4). Mice with bile duct ligation to induce cholestatic disease also demonstrate analgesia to mechanical stimulation of the paw (5). However, the mechanisms of cholestatic itch and painless jaundice are unknown.

The distinct sensations of itch and pain are evoked by different stimuli that elicit the discrete responses of scratching and withdrawal (6). Itch and pain are antagonistic: painful stimuli (scratching) relieve itch (7), and analgesics (intrathecal morphine) can cause itch (8). However, itch and pain are related because they both protect against irritating and damaging stimuli, and they share a similar mechanism of transmission: pruritogens and algesic substances are sensed in the skin by primary spinal afferent neurons of the dorsal root ganglia (DRG), which transmit information to the brain via second-order neurons in the dorsal horn of the spinal cord (6). Whether itch and pain are transmitted by the same or different neurons is uncertain. The labeled line hypothesis proposes that there are distinct populations of neurons that transmit either itch or pain. The existence of an itch-specific pathway was supported by the identification of histamine-selective C fibers in human skin (9), and by the report that gastrin-releasing peptide (GRP) is an itch-selective transmitter of DRG neurons (10) that activates the GRP receptor (GRPR) on spinal neurons, which transmit itch but not pain (11). A heterodimer of the GRPR and a μ-opioid receptor (MOR) variant, MOR1D, in spinal neurons may mediate opioid-induced itch (12). However, sensory nerves in the skin are selective but not specific for histamine, since they also respond to nociceptive stimuli such as capsaicin (13), an agonist of the transient receptor potential vanilloid 1 channel (TRPV1), and DRG nociceptors expressing TRPV1 are necessary for scratching behavior (14). Mice lacking vesicular glutamate transporter 2 in subsets of DRG neurons exhibit attenuated pain but enhanced itch (15, 16), which implicates this transporter in both sensations. These findings support the selectivity theory of itch, which proposes that primary spinal afferent neurons can sense both pruritogens and algesic substances and that inactivation of central pain signaling is a prerequisite for itch transmission (6, 17).

Peripheral and central mechanisms may explain the itch and analgesia that can accompany liver disease. Bile acids (BAs) are potential mediators, since cholestatic patients have increased BA concentrations in the circulation (18) and skin (19), and application of BAs to the skin causes itch (20, 21), whereas bile salt–binding resins relieve cholestatic pruritus (22). Alterations in opioids

Authorship note: Farzad Alemi and Edwin Kwon are co–first authors.

Conflict of interest: The authors have declared that no conflict of interest exists.

Citation for this article: *J Clin Invest.* 2013;123(4):1513–1530. doi:10.1172/JCI64551.

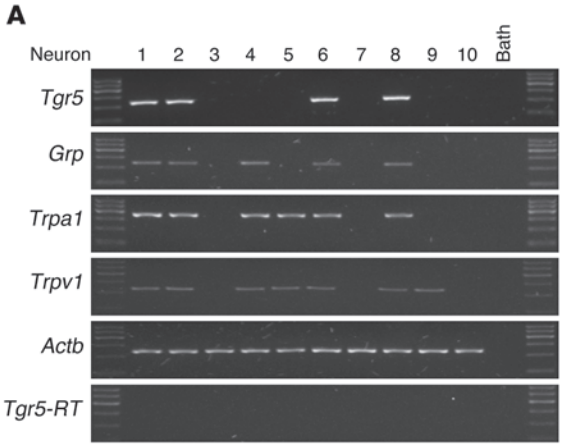
A
Neuron
1
2
3
4
5
6
7
8
9
10
Bath
Tgr5
Grp
Trpa1
Trpv1
Actb
Tgr5-RT

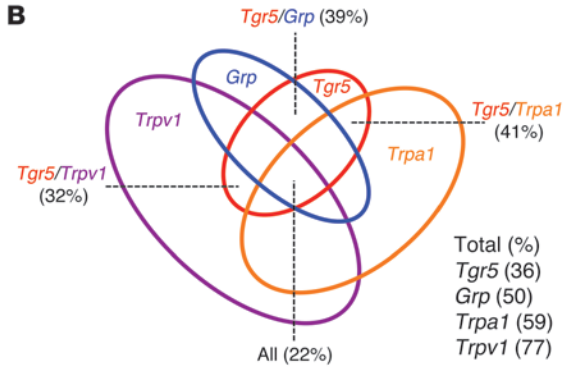
B
Tgr5/Grp (39%)
Grp
Tgr5
Trpv1
Tgr5/Trpa1
(41%)
Trpa1
Tgr5/Trpv1
(32%)
All (22%)
Total (%)
Tgr5 (36)
Grp (50)
Trpa1 (59)
Trpv1 (77)

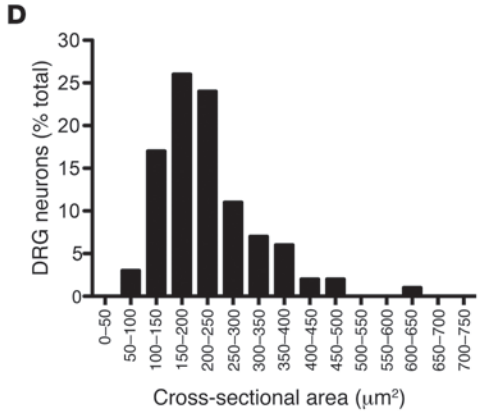
D
DRG neurons (% total)
30
25
20
15
10
5
0
0–50
50–100
100–150
150–200
200–250
250–300
300–350
350–400
400–450
450–500
500–550
550–600
600–650
650–700
700–750
Cross-sectional area (μm²)

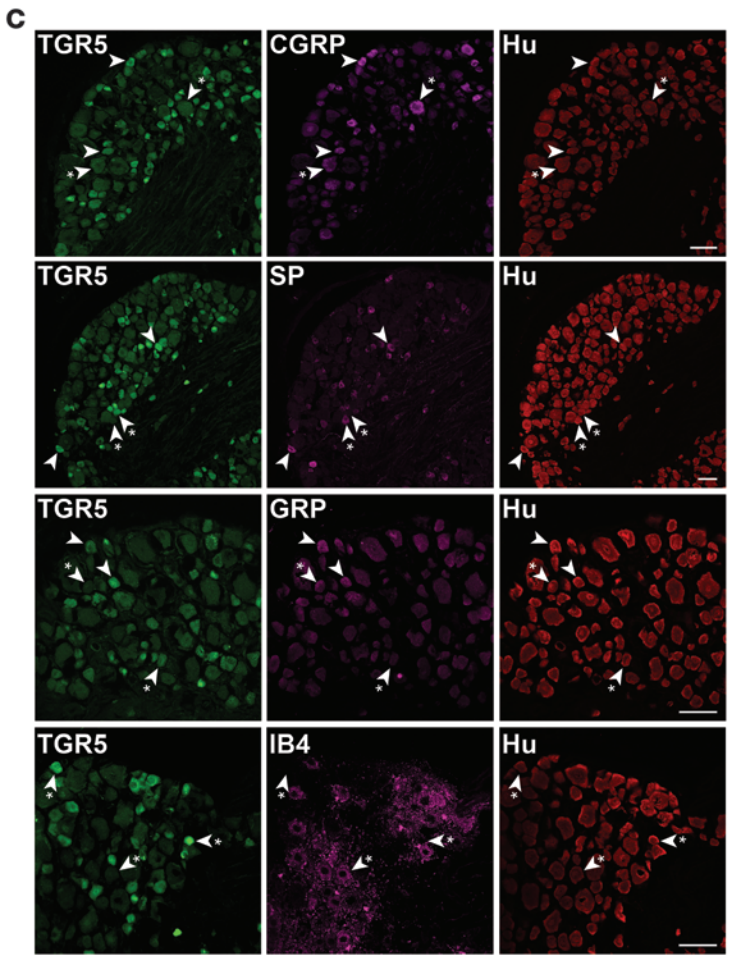
C
TGR5
CGRP
Hu
TGR5
SP
Hu
TGR5
GRP
Hu
TGR5
IB4
Hu

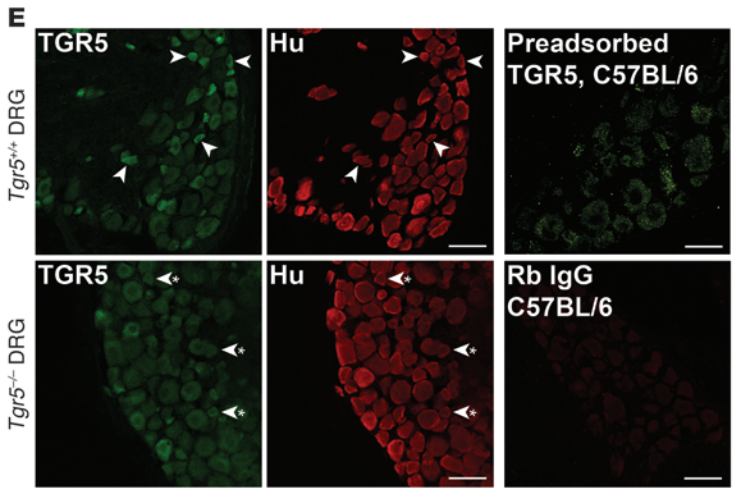
E
Tgr5+/+ DRG
TGR5
Hu
Preadsorbed
TGR5, C57BL/6
Tgr5−/− DRG
TGR5
Hu
Rb IgG
C57BL/6

Figure 1
TGR5 expression and localization in mouse DRG. (**A**) Single-cell RT-PCR analysis of DRG neurons from C57BL/6 mice. Small-diameter neurons were selected, and *Tgr5*, *Grp*, *Trpa1*, and *Trpv1* mRNA was amplified. Results from 10 neurons are shown (78 neurons, 7 mice). Neurons 1, 2, 6, and 8 coexpressed *Tgr5*, *Grp*, *Trpa1*, and *Trpv1*. No transcripts were amplified from bath fluid. (**B**) Proportion of small-diameter neurons expressing *Tgr5* (36%), *Grp* (50%), *Trpa1* (59%), and *Trpv1* (77%). Of the *Tgr5*-expressing neurons, 39% coexpressed *Grp*, 41% coexpressed *Trpa1*, and 32% coexpressed *Trpv1*. *Tgr5*, *Grp*, *Trpa1*, and *Trpv1* were all coexpressed by 22% of small-diameter neurons. (**C**) Localization of TGR5-IR, Hu-IR, CGRP-IR, SP-IR, GRP-IR, and IB4-FITC binding in DRG (thoracic, lumbar, and sacral) of C57BL/6 mice. Arrowheads denote neurons coexpressing markers; arrowheads with asterisks denote lack of marker coexpression. TGR5-IR was prominently expressed in small-diameter Hu-positive neurons, most of which coexpressed CGRP-IR, SP-IR, or GRP-IR. TGR5-IR was rarely expressed in neurons that bound IB4-FITC. (**D**) Cross-sectional area of the TGR5-IR population (50-μm^2 bins), which indicated that 50% of TGR5-IR neurons were 150–250 μm^2. (**E**) Controls for specific detection of TGR5-IR. TGR5-IR was prominently detected in small-diameter DRG neurons of *Tgr5*-WT mice (arrowheads). TGR5-IR of small-diameter neurons of *Tgr5*-KO mice was markedly diminished (arrowheads with asterisks), although the background fluorescence of larger-diameter neurons was retained. Preadsorption of the TGR5 antibody with the receptor fragment used for immunization abolished TGR5-IR in DRG of C57BL/6 mice. There was no staining when the primary antibody was replaced with normal rabbit (Rb) IgG. Scale bars: 50 μm.

and their receptors may also contribute. There are increased circulating levels of opioids in humans (23) and rats (24) with cholestatic disease, and fewer MOR binding sites in the brain of cholestatic rats (25). The opioid antagonist naloxone can alleviate cholestatic pruritus (26) and reverses the analgesia observed in mice with cholestasis (5). However, the mechanisms by which sensory nerves detect and respond to BAs are unknown, and the neuronal mediators of BA-induced itch and analgesia have not yet been identified.

In addition to their role in the digestion and absorption of dietary fats, BAs are signaling molecules that regulate multiple cell types by activating nuclear and plasma membrane receptors (27). We report a major role for TGR5 (also known as GPR131 or GpBAR1), a G protein–coupled plasma membrane receptor for BAs (28, 29), in BA-induced itch and analgesia. TGR5 is a widely distributed receptor that has been implicated in energy metabolism (30), glucose homeostasis (31, 32), bile composition/secretion (33–36), and inflammation (28, 37, 38). TGR5 is also expressed by neurons of the enteric and central nervous systems, where it may mediate the effects of BAs on intestinal motility (39) and detect endogenous neurosteroids (40, 41). The existence of TGR5 in the nervous system led us to hypothesize that TGR5 on sensory nerves mediates BA-induced itch and analgesia.

Results

TGR5 is expressed by peptidergic neurons of the DRG. In order to determine whether TGR5 is expressed by DRG neurons involved in itch and pain, small-diameter neurons (<25 μm) from mouse (C57BL/6) DRG (all regions) were individually selected, and expression of *Tgr5* mRNA was examined by single-cell nested PCR. Neurons were further characterized by similarly examining the expression of mRNA for the itch transmitter *Grp* (10, 42) and for the *Trpa1* and *Trpv1* ion channels that participate in itch and pain transmission (14, 43, 44). Transcripts corresponding in size to *Tgr5* (236 bp) were amplified from 36% of small-diameter DRG neurons (78 neurons from 7 mice; Figure 1, A and B). Of all of the small-diameter neurons, 50% expressed *Grp* (206 bp), 59% expressed *Trpa1* (393 bp), and 77% expressed *Trpv1* (229 bp) (Figure 1B). Of the *Tgr5*-expressing neurons, 39% coexpressed *Grp*, 41% coexpressed *Trpa1*, and 32% coexpressed *Trpv1*. *Tgr5*, *Grp*, *Trpa1*, and *Trpv1* were all coexpressed by 22% of small-diameter neurons. The identity of all transcripts was confirmed by sequencing, and no products were amplified from the neuronal culture medium or when RT was omitted.

Using an antibody raised in rabbit to the carboxyl terminus of human TGR5 (39), we found TGR5 to be localized to DRG neurons (thoracic, lumbar, and sacral). The neuronal subtypes expressing TGR5 were characterized by simultaneous localization of TGR5 with the pan-neuronal marker Hu (human antibody), and with neuropeptide transmitters of itch (GRP, goat antibody) and neurogenic inflammation and pain (calcitonin gene–related peptide [CGRP], sheep antibody, and substance P [SP], rat antibody). Nonpeptidergic neurons were identified by examining binding of isolectin B4 (IB4) conjugated to FITC. TGR5 immunoreactivity (TGR5-IR) was prominently localized to small-diameter neurons, with a cross-sectional area of 150–250 μm^2 (Figure 1, C and D). Of the Hu-IR neurons, 28% coexpressed TGR5-IR (259 TGR5-IR of 931 Hu-IR neurons from 5 mice). All of the TGR5-IR cells coexpressed Hu-IR (259 of 259 neurons, 100%), and were thus confirmed to be neurons. The TGR5-IR neurons were mostly peptidergic (Figure 1C). Of all of the TGR5-IR neurons, 38% coexpressed CGRP (133 of 248) and 48% coexpressed SP (188 of 393). Of the CGRP-IR neurons, 63% coexpressed TGR5-IR (123 of 194), and of the SP-IR neurons, 66% coexpressed TGR5-IR (188 of 286). GRP-IR also colocalized with TGR5-IR in small-diameter DRG neurons (Figure 1C). However, there was considerable variability in the intensity of the GRP-IR between neurons, which precluded quantification of the extent of GRP-IR and TGR5-IR colocalization. TGR5 was not prominently colocalized with nonpeptidergic neurons that bound IB4-FITC (Figure 1C). Of the TGR5-IR neurons, only 8% bound IB4-FITC (15 of 193), and of the neurons that bound IB4-FITC, only 9% expressed TGR5-IR (15 of 176). TGR5-IR was also present in peptidergic neurons that coexpressed SP or CGRP in rat DRG (data not shown).

The TGR5 antibody specifically interacts with human TGR5 expressed in HEK293 cells (39). In order to further characterize specificity in mice, we compared DRG sections from *Tgr5*-WT and *Tgr5*-KO mice. The TGR5 antibody strongly stained small-diameter neurons of *Tgr5*-WT mice (Figure 1E). In contrast, the staining of small-diameter neurons of *Tgr5*-KO mice was markedly diminished, although the background fluorescence of larger-diameter neurons was retained (Figure 1E). Expression of Hu-IR, SP-IR, CGRP-IR, and GRP-IR was the same in *Tgr5*-WT and *Tgr5*-KO mice (Figure 1E and data not shown). Preadsorption of the TGR5 antibody with the receptor fragment that was used for immunization abolished the TGR5-IR signal in DRG neurons from *Tgr5*-WT and C57BL/6 mice (Figure 1E). Staining was also absent when the TGR5 antibody was replaced with normal rabbit IgG or was omitted (Figure 1E and data not shown). These results indicate that the TGR5 antibody specifically detects TGR5 in mouse DRG neurons.

As a control for the specific detection of GRP in DRG neurons, sections of mouse DRG and gastric antrum, where GRP is found

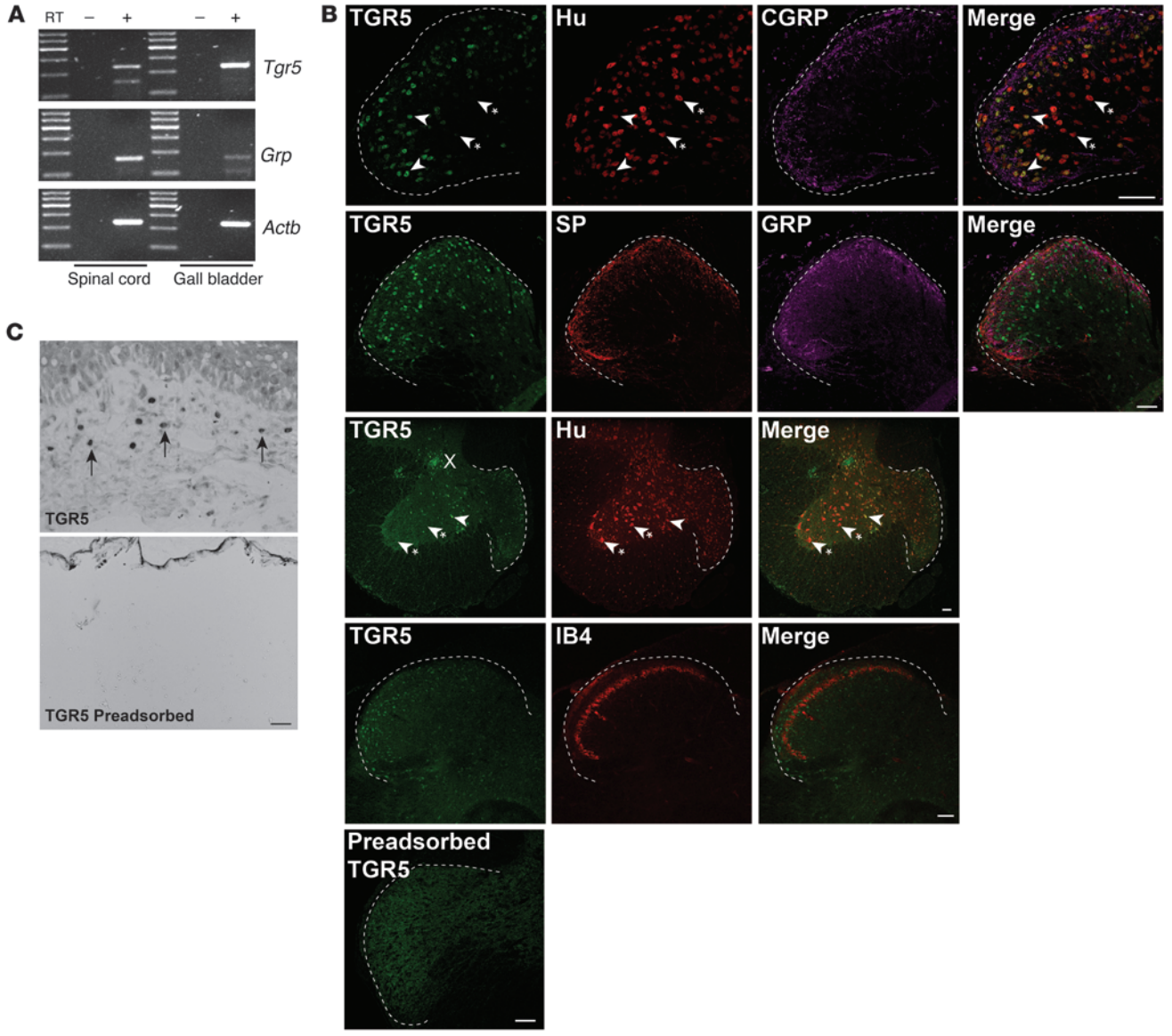

Figure 2
Expression and localization of TGR5 in mouse spinal cord and skin. (**A**) Amplification of *Tgr5* and *Grp* from mouse spinal cord and gall bladder. Shown are representative gels from 3 or 4 mice. (**B**) Localization of TGR5-IR, Hu-IR, CGRP-IR, SP-IR, GRP-IR, and IB4-FITC binding in the dorsal horn (dashed outline) of the spinal cord (sacral and lumbar) of C57BL/6 mice. Arrowheads denote neurons coexpressing markers; arrowheads with asterisks denote lack of marker coexpression. TGR5-IR was prominently localized in Hu-positive neurons in laminae I, II, and X. There was no clear colocalization of TGR5-IR with CGRP-IR, SP-IR, GRP-IR, or IB4-FITC in nerve fibers. Preadsorption of the TGR5 antibody abolished staining. (**C**) In mouse skin, TGR5-IR localized to dermal macrophages (arrows), which were identified based on appearance and location. Preadsorption of the TGR5 antibody with the receptor fragment used for immunization abolished TGR5-IR in spinal neurons and dermal macrophages. Scale bars: 50 μm.

in enteric nerves that control gastrin secretion, were incubated with the GRP antibody used for neurochemical coding (goat) and a well-characterized antibody that was raised in rabbits (45). Both antibodies stained the same DRG neurons, and both stained neurons of the myenteric plexus and mucosal nerve fibers of the gastric antrum (Supplemental Figure 1; supplemental material available online with this article; doi:10.1172/JCI64551DS1). The goat GRP antibody clearly stained myenteric neurons and fibers in a whole-mount preparation of the gastric antrum. These results indicate that *Tgr5* mRNA and TGR5-IR are expressed by small-diameter peptidergic neurons containing CGRP, SP, and GRP that also express TRPA1 and TRPV1.

TGR5 is expressed by spinal neurons and dermal macrophages. The expression of TGR5 and GRP was examined in whole spinal cord (all regions) of C57BL/6 mice by RT-PCR. Transcripts corresponding to *Tgr5* (236 bp) and *Grp* (206 bp) mRNA were amplified from the spinal cord, and *Tgr5* mRNA was also amplified from the gall bladder, an established site of TGR5 expression that was used as a positive control (Figure 2A). Segments of spinal cord (sacral and lumbar) of C57BL/6 mice were stained to detect TGR5-IR, Hu-IR,

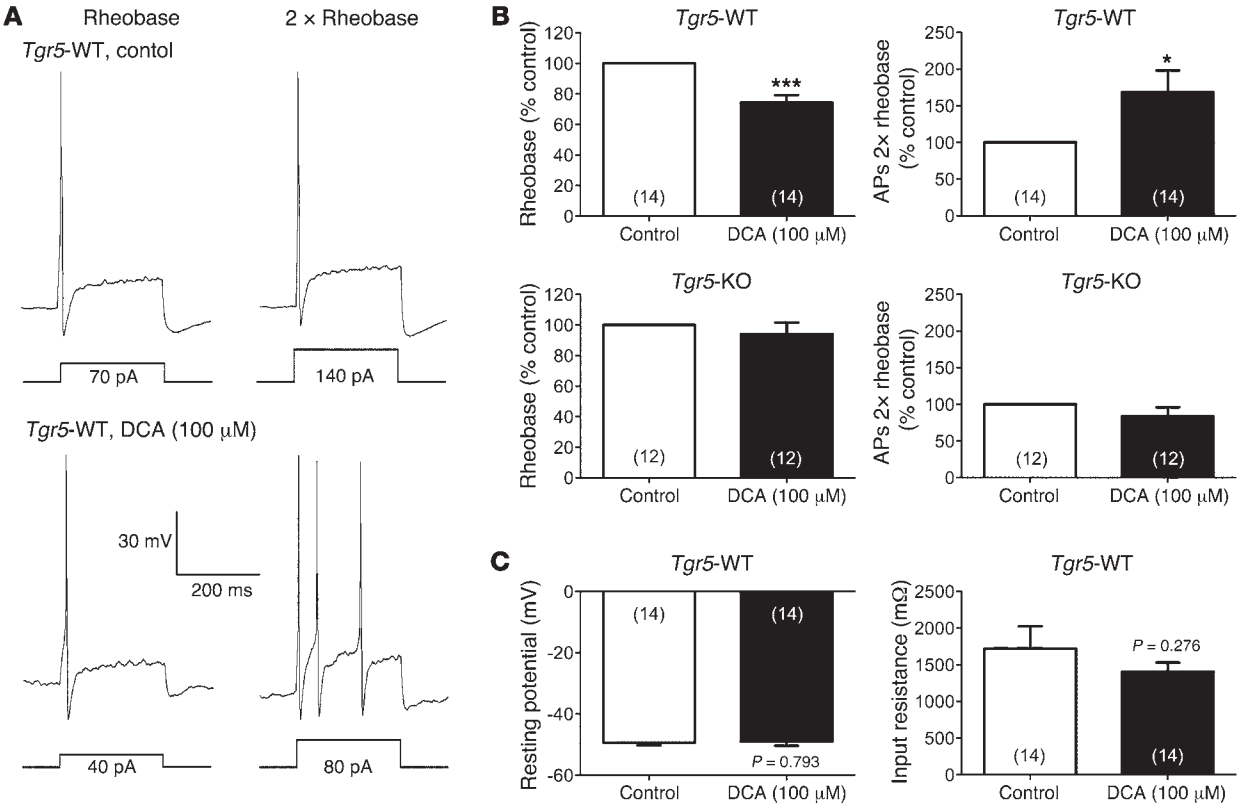

Figure 3

Effects of DCA on intrinsic excitability of DRG neurons from *Tgr5*-WT and *Tgr5*-KO mice. (**A**) Representative perforated current clamp recordings in response to 500 ms current injection at rheobase (left) and 2× rheobase (right). Recordings were made from the same neuron from a *Tgr5*-WT mouse before (control; top) and after (bottom) incubation with DCA (100 μM, 10 minutes). Square waves represent the electrical stimulus applied to the cell (500 ms). (**B**) Summary data showing rheobase and AP discharge frequency at 2× rheobase of neurons from *Tgr5*-WT and *Tgr5*-KO mice. Recordings were made before (control) and after incubation with DCA (100 μM, 10 minutes). Rheobase and AP discharge frequency were normalized to control values to account for variability in control responses between experiments. DCA decreased rheobase and increased AP discharge frequency at 2× rheobase in neurons from *Tgr5*-WT mice, but had no effect on neurons from *Tgr5*-KO mice. (**C**) Summary data showing that DCA did not affect resting membrane potential or input resistance of neurons from *Tgr5*-WT mice. $^{*}P < 0.05$, $^{***}P < 0.005$ vs. control; paired *t* test. The number of neurons is indicated in parenthesis in each bar. Neurons were obtained from ≥3 mice.

and markers of peptidergic (CGRP-IR, SP-IR, GRP-IR) and non-peptidergic (IB4-FITC binding) neurons. TGR5-IR was detected in a subpopulations of Hu-IR neurons of laminae I, II, and V of the dorsal horn, and lamina X in the region of the central canal (Figure 2B). TGR5-IR was prominently localized in neuronal cell bodies, whereas CGRP-IR, SP-IR, GRP-IR, and IB4-FITC were detected in nerve fibers in the dorsal horn. In order to examine the localization of TGR5 in peripheral tissues, sections of mouse skin were studied. TGR5-IR was detected in dermal macrophages, which were identified by histological appearance (Figure 2C). Preadsorption of the TGR5 antibody with the immunizing peptide abolished staining in the spinal cord and the skin (Figure 2, B and C), confirming specific detection of TGR5. These results indicate that TGR5 is expressed by a subpopulation of spinal neurons and by dermal macrophages that are known to contain opioids (46). Attempts to simultaneously localize TGR5 and opioids were unsuccessful due to the inadequacy of the available opioid antibodies raised in species appropriate for simultaneous localization.

BAs and a TGR5-selective agonist increase the intrinsic excitability of DRG neurons by a TGR5-dependent mechanism. In order to determine whether BAs can directly regulate the excitability of primary spinal afferent neurons, patch-clamp recordings were made from acutely dissociated mouse DRG neurons. Recordings were made from small-diameter neurons (<30 pF capacitance), because these neurons possess the properties of nociceptors (e.g., sensitivity to capsaicin; ref. 47). The intrinsic excitability of neurons was assessed by measurement of the rheobase (minimal input current required to generate 1 action potential [AP]) and the AP discharge frequency at a current twice that of rheobase (2× rheobase). Input currents were applied for 500 ms. Recordings were made from neurons before (basal control) and after incubation with BAs or a TGR5-selective agonist (all 10, 30, or 100 μM, 10 minutes) or vehicle control (1% DMSO, 0.9% NaCl).

Incubation of DRG neurons from *Tgr5*-WT mice with deoxycholic acid (DCA; 100 μM, 10 minutes), which activates TGR5 (28, 29), caused a 28% decrease in rheobase (control, 108.6 ± 16.0 pA; DCA, 77.9 ± 9.8 pA; $P = 0.002$) and a 63% increase in AP discharge frequency at 2× rheobase (control, 1.6 ± 0.3 APs during 500-ms input current; DCA, 2.6 ± 0.5 APs; $P = 0.015$) (Figure 3, A and B). In marked contrast, DCA did not affect rheobase or AP discharge frequency of neurons from *Tgr5*-KO mice (Figure 3B). DCA had no effect on the resting membrane potential or the input resis-

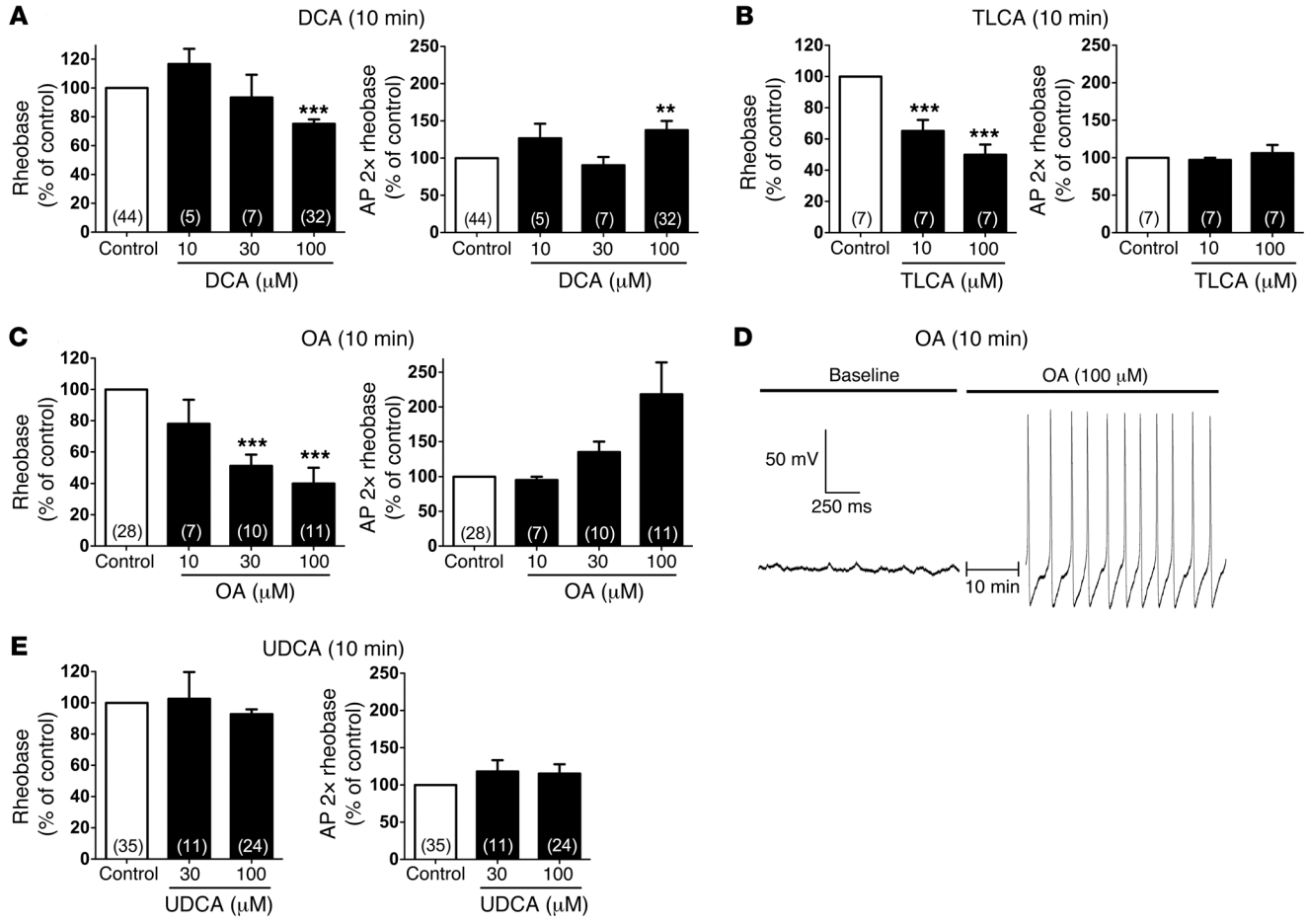

Figure 4

Effects of graded concentrations of BAs and a TGR5 agonist on intrinsic excitability of DRG neurons from C57BL/6 mice. (**A**–**C** and **E**) Summary data showing rheobase and AP discharge frequency at 2× rheobase. Recordings were made before (control) and after incubation with DCA (**A**), TLCA (**B**), OA (**C**), or UDCA (**E**) (10, 30, or 100 μM, 10 minutes). Rheobase and AP discharge frequency were normalized to control values to account for variability in control responses between experiments. DCA (100 μM) decreased rheobase and increased AP discharge frequency, whereas TLCA (10 and 100 μM) only decreased rheobase. OA caused a robust and concentration-dependent decrease in rheobase and increase in AP discharge frequency. UDCA had no effect on rheobase or AP discharge frequency. (**D**) Representative recording of the membrane potential of a neuron immediately before and after incubation with OA (100 μM, 10 minutes). OA exposure resulted in spontaneous AP discharge (no input current). $^{**}P < 0.001$, $^{***}P < 0.0001$ vs. control, 1-way ANOVA and Dunnett post-hoc test. The number of neurons is indicated in parenthesis in each bar. Neurons were obtained from ≥3 mice.

tance of neurons from *Tgr5*-WT mice (Figure 3C). Vehicle control treatment did not affect rheobase, AP discharge frequency, resting membrane potential, or input resistance (data not shown). Thus, DCA increased the intrinsic excitability of DRG neurons in a TGR5-dependent manner, but did not directly depolarize neurons.

To further characterize the effects of BAs on neuronal excitability, DRG neurons from C57BL/6 mice were incubated with graded concentrations of BAs that are known to activate TGR5, including DCA and taurolithocholic acid (TLCA) (28, 29). Although the highest concentration of DCA (100 μM, 10 minutes) reduced rheobase and increased AP discharge frequency at 2× rheobase, lower concentrations of DCA (10 or 30 μM) had no effect (Figure 4A). TLCA (10 or 100 μM, 10 minutes) reduced rheobase but did not affect AP discharge frequency (Figure 4B). Oleanolic acid (OA) is a naturally occurring component of leaves from the olive tree *Olea europaea* that potently activates TGR5, but not the nuclear farnesoid X BA receptor (48). OA (10, 30, or 100 μM, 10 minutes) caused a concentration-dependent decrease in rheobase and increase in AP discharge frequency (Figure 4C). The highest concentration of OA (100 μM) decreased rheobase to 40.0% ± 9.9% of control and increased AP discharge frequency to 218.2% ± 46% of control. Further evidence in support of increased excitability was the observation that 36% of neurons treated with 100 μM OA exhibited spontaneous AP discharge and anodal break excitation compared with control (4 of 11, $P = 0.024$), an effect not seen with DCA or TLCA (Figure 4D). This increased excitability of OA-treated neurons was associated with an increase in the input resistance (basal, 1,078 ± 224 mΩ; OA, 1,625 ± 230 mΩ; $P = 0.045$), suggesting closure of K^+ channels. In contrast, DCA and TLCA did not affect the input resistance or the resting membrane potential (Figure 3C and data not shown). Ursodeoxycholic acid (UDCA) has been reported either to not activate TGR5 or to have weak agonis-

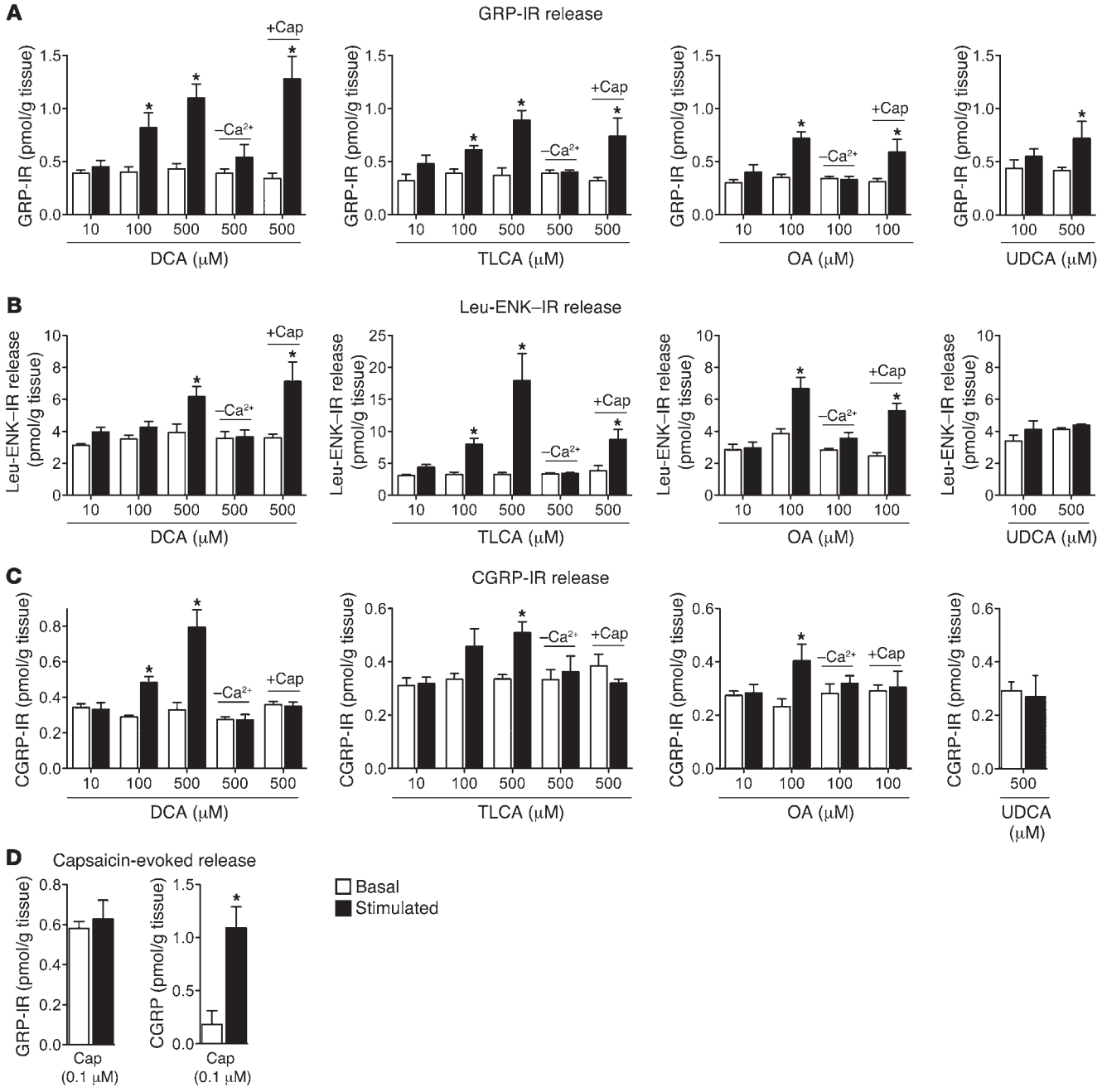

Figure 5

Effects of BAs, a TGR5-selective agonist, and capsaicin on GRP-IR, Leu-ENK–IR, and CGRP-IR release from rat spinal cord with attached dorsal roots. Release of GRP-IR (**A**), Leu-ENK–IR (**B**), and CGRP-IR (**C**) was measured from superfused segments of rat spinal cord with attached dorsal roots (combined cervical, thoracic, and lumbar-sacral regions) under basal conditions and after superfusion with DCA, TLCA, OA, or UDCA (10, 100, and/or 500 μM, 60 minutes superfusion). DCA, TLCA, and OA stimulated GRP-IR, Leu-ENK–IR, and CGRP-IR release over basal. UDCA stimulated GRP-IR release only at the highest concentration (500 μM). Removal of extracellular calcium ($–Ca^{2+}$) prevented DCA-, TLCA- and OA-stimulated release. Preincubation with capsaicin (+Cap) did not affect DCA-, TLCA-, or OA-evoked GRP-IR or Leu-ENK–IR release, but prevented CGRP-IR release. (**D**) Capsaicin did not stimulate GRP-IR release, but strongly stimulated CGRP-IR release. *$P < 0.05$ vs. basal in the same tissue; paired *t* test. $n = 4–5$.

tic activity, while retaining the detergent and irritant properties of BAs (28, 49). UDCA (30 or 100 μM, 10 minutes) did not affect rheobase, AP discharge frequency, resting membrane potential, or input resistance (Figure 4E and data not shown). These results demonstrated that BAs known to potently activate TGR5 (DCA and TLCA) and a TGR5-selective agonist (OA) directly regulated the intrinsic excitability of small-diameter DRG neurons that participate in itch and pain transmission.

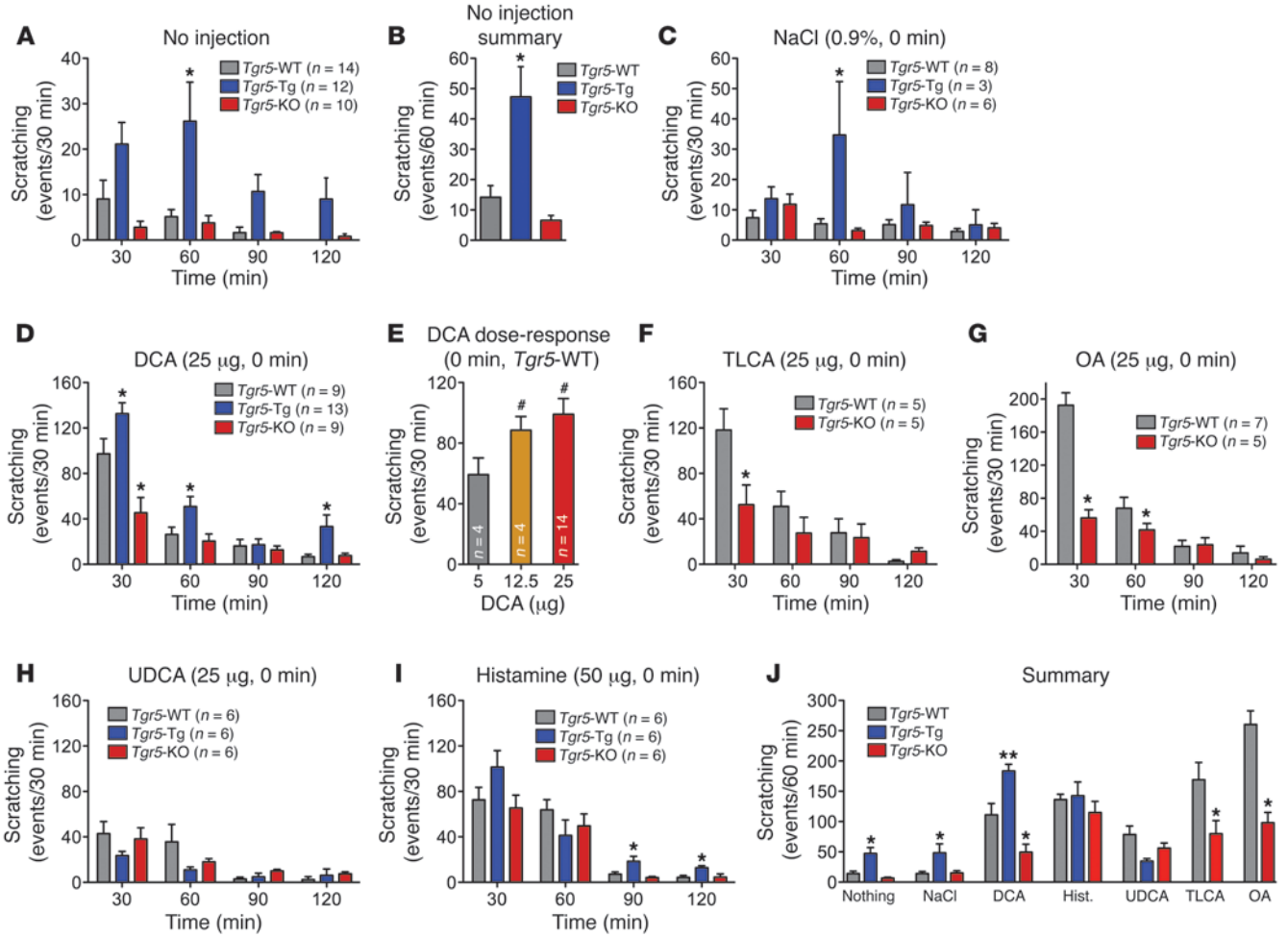

Figure 6

Effects of BAs on scratching behavior in *Tgr5*-WT, *Tgr5*-KO, and *Tgr5*-Tg mice. Results are expressed as the number of scratching events for the indicated time periods. (**A** and **B**) Spontaneous scratching in untreated mice. (**A**) Frequency of spontaneous scratching events during 30-minute intervals over 120 minutes of recording. (**B**) Frequency of spontaneous scratching events per 60 minutes, averaged over 120 minutes of recording. *Tgr5*-Tg mice exhibited increased frequency of spontaneous scratching compared with *Tgr5*-WT and *Tgr5*-KO mice. (**C**) Vehicle control (0.9% NaCl, intradermal to the nape of the neck) did not stimulate scratching, although scratching was generally more frequent in *Tgr5*-Tg mice. (**D**) DCA (25 μg, intradermal) robustly stimulated scratching in *Tgr5*-WT mice, and scratching was exacerbated in *Tgr5*-Tg mice and suppressed in *Tgr5*-KO mice. (**E**) DCA (5–25 μg) stimulated dose-dependent scratching in *Tgr5*-WT mice. (**F** and **G**) TLCA and OA (25 μg) stimulated scratching in *Tgr5*-WT mice, which was markedly attenuated in *Tgr5*-KO mice. (**H**) UDCA (25 μg) had a small stimulatory effect that was not different among *Tgr5*-Tg, *Tgr5*-KO, and *Tgr5*-WT mice. (**I**) Histamine (50 μg) stimulated scratching to a similar extent in *Tgr5*-Tg, *Tgr5*-KO, and *Tgr5*-WT mice. (**J**) Summarized results showing the frequency of scratching events during the first 60 minutes after injection. $^{*}P < 0.05$, $^{**}P < 0.01$ vs. *Tgr5*-WT; $^{\#}P < 0.05$ vs. 5 μg DCA; ANOVA and Student-Newman-Keuls post-hoc test. *n* is indicated.

BAs and a TGR5-selective agonist stimulate release of neuropeptide transmitters of itch and analgesia. GRP is an itch-selective transmitter (10, 11), and leucine-enkephalin (Leu-ENK) induces both itch and analgesia (5, 26). GRP has been detected in DRG and spinal cord (10, 42, 50), and Leu-ENK is present in the spinal cord (51). To assess whether TGR5 regulates release of these neuropeptides, segments of spinal cord with attached dorsal roots were superfused with BAs and a TGR5-selective agonist (10, 100, or 500 μM, 60 minutes superfusion), and neuropeptide release was measured by ELISA. It was necessary to study neuropeptide release from rats rather than mice, since only rats provided sufficient tissue for detection of the low concentrations of secreted neuropeptides.

DCA and TLCA stimulated concentration-dependent release of GRP-IR and Leu-ENK–IR (Figure 5, A and B). The maximal responses were to DCA (500 μM), which caused a 3-fold increase over basal in GRP-IR release (1.33 ± 0.05 vs. 0.45 ± 0.09 pmol/g; $P = 0.001$), and TLCA (500 μM), which caused a 7-fold increase over basal in Leu-ENK–IR release (21.60 ± 6.24 vs. 3.08 ± 0.43 pmol/g; $P = 0.042$). However, lower concentrations (100 μM) of both BAs also significantly stimulated release of GRP-IR and Leu-ENK–IR. DCA and TLCA did not release GRP-IR and Leu-ENK–IR in the absence of extracellular calcium (Figure 5, A and B). OA also stimulated calcium-dependent release of GRP-IR and Leu-ENK–IR (Figure 5, A and B). UDCA did not stimulate GRP-IR release, except at high concentrations (500 μM) (Figure 5A).

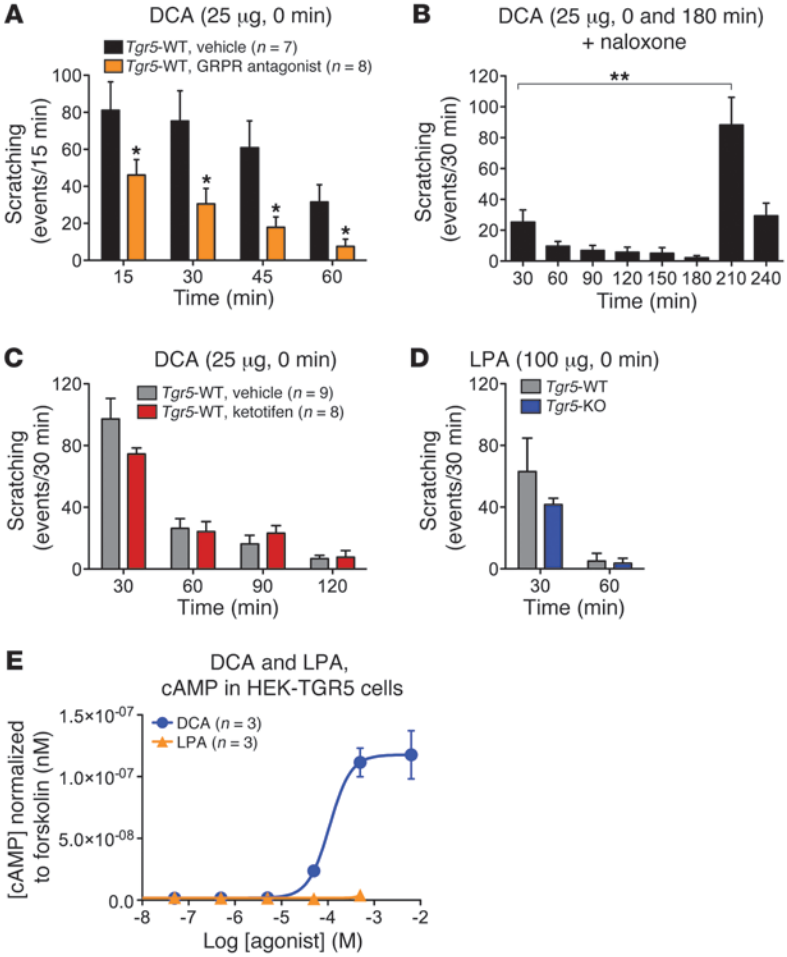

Figure 7
Mechanisms of BA-stimulated scratching in mice. (**A**) The GRPR antagonist [Tyr^4, D-Phe^{12}]-bombesin or vehicle (control) were injected intrathecally 10 minutes before intradermal injection of DCA (25 μg) to *Tgr5*-WT mice. GRPR antagonist attenuated DCA-stimulated scratching at all time points compared with vehicle. (**B**) Naloxone was administered intravenously 30 minutes before the first intradermal injection of DCA into *Tgr5*-WT mice (at 0 minutes). Naloxone attenuated the scratching response to the first DCA challenge. DCA administered at 180 minutes, when naloxone was cleared, strongly stimulated scratching. (**C**) Ketotifen or vehicle was administered intravenously 5 minutes before intradermal injection of DCA (25 μg) to *Tgr5*-WT mice. Ketotifen had no effect on the scratching response to DCA. (**D**) LPA (100 μg) was injected intradermally. Scratching frequency was similar in *Tgr5*-WT and *Tgr5*-KO mice. (**E**) cAMP generation in HEK293 cells expressing human TGR5. DCA stimulated concentration-dependent cAMP formation, whereas LPA did not stimulate cAMP generation ($n = 3$ experiments, in triplicate). *$P < 0.05$ vs. vehicle, **$P < 0.01$ as indicated; unpaired *t* test. *n* is indicated.

Although it does not cause pruritus in human skin (52), CGRP is a mediator of neurogenic inflammation that colocalizes with GRP in DRG neurons (10). DCA, TLCA, and OA, but not UDCA, stimulated calcium-dependent release of CGRP-IR from the spinal cord and DRG (Figure 5C).

The neuropeptides released from segments of spinal cord with attached dorsal roots may derive from spinal neurons or from the central projections of DRG neurons within the dorsal horn. To determine whether BAs stimulate neuropeptide release from DRG neurons that express TRPV1, tissues were preincubated with capsaicin (10 μM, 20 minutes). This treatment can deplete neuropeptides such as CGRP from primary spinal afferent neurons expressing TRPV1. Preincubation with capsaicin did not affect DCA-, TLCA- or OA-evoked release of GRP-IR or Leu-ENK–IR (Figure 5, A and B). In marked contrast, capsaicin preincubation prevented DCA-, TLCA-, and OA-evoked release of CGRP-IR (Figure 5C). In keeping with these results, capsaicin (0.1 μM) did not affect GRP-IR release, but strongly stimulated CGRP-IR release (Figure 5D). These findings indicate that BAs known to activate TGR5 and a TGR5-selective agonist can stimulate release of neuropeptides from the spinal cord and DRG of rats. GRP-IR and Leu-ENK–IR probably derived from spinal neurons, since preincubation with capsaicin did not affect BA-evoked release of these neuropeptides, and direct stimulation with capsaicin had no effect on GRP-IR release. In contrast, CGRP-IR derived from TRPV1-expressing primary spinal afferent neurons, since capsaicin preincubation prevented BA-evoked CGRP-IR release, and capsaicin directly stimulated CGRP release.

BAs activate TGR5 and induce GRP- and opioid-mediated itch. To determine whether BAs induce itch by a TGR5-dependent mechanism, scratching behavior was examined in *Tgr5*-WT and *Tgr5*-KO mice as well as in *Tgr5*-Tg mice (overexpressing mouse TGR5). Test agents were injected intradermally into the nape of the neck, and scratching events (movement of hind limb to injection site) were recorded.

Without injection, *Tgr5*-WT mice exhibited a low frequency of spontaneous scratching (14.2 ± 3.8 events/60 minutes; Figure 6, B and J). This frequency increased 3.4-fold in *Tgr5*-Tg mice (47.3 ± 1.6 events/60 minutes; $P = 0.037$, *Tgr5*-Tg vs. *Tgr5*-WT), which was 7-fold higher than in *Tgr5*-KO mice (6.6 ± 1.6 events/60 minutes; $P = 0.021$, *Tgr5*-Tg vs. *Tgr5*-KO). Scratching events measured within 60 minutes of vehicle (0.9% NaCl) injection similarly increased 3.5-fold in *Tgr5*-Tg and *Tgr5*-WT mice ($P = 0.011$; Figure 6, C and J).

In *Tgr5*-WT mice, intradermal injection of DCA (25 μg) strongly stimulated scratching within 30 minutes (DCA, 97.2 ± 13.3 events/30 minutes; control, 4.5 ± 2.1 events/30 minutes), which declined to baseline within 90–120 minutes (Figure 6, D and J). Compared with *Tgr5*-WT controls, DCA-induced scratching was diminished in *Tgr5*-KO mice (45.4 ± 13.4 events/30 minutes; $P = 0.001$), but amplified in *Tgr5*-Tg mice (132.6 ± 9.7 events/30 minutes; $P = 0.001$; Figure 6D). The effects of DCA were dose

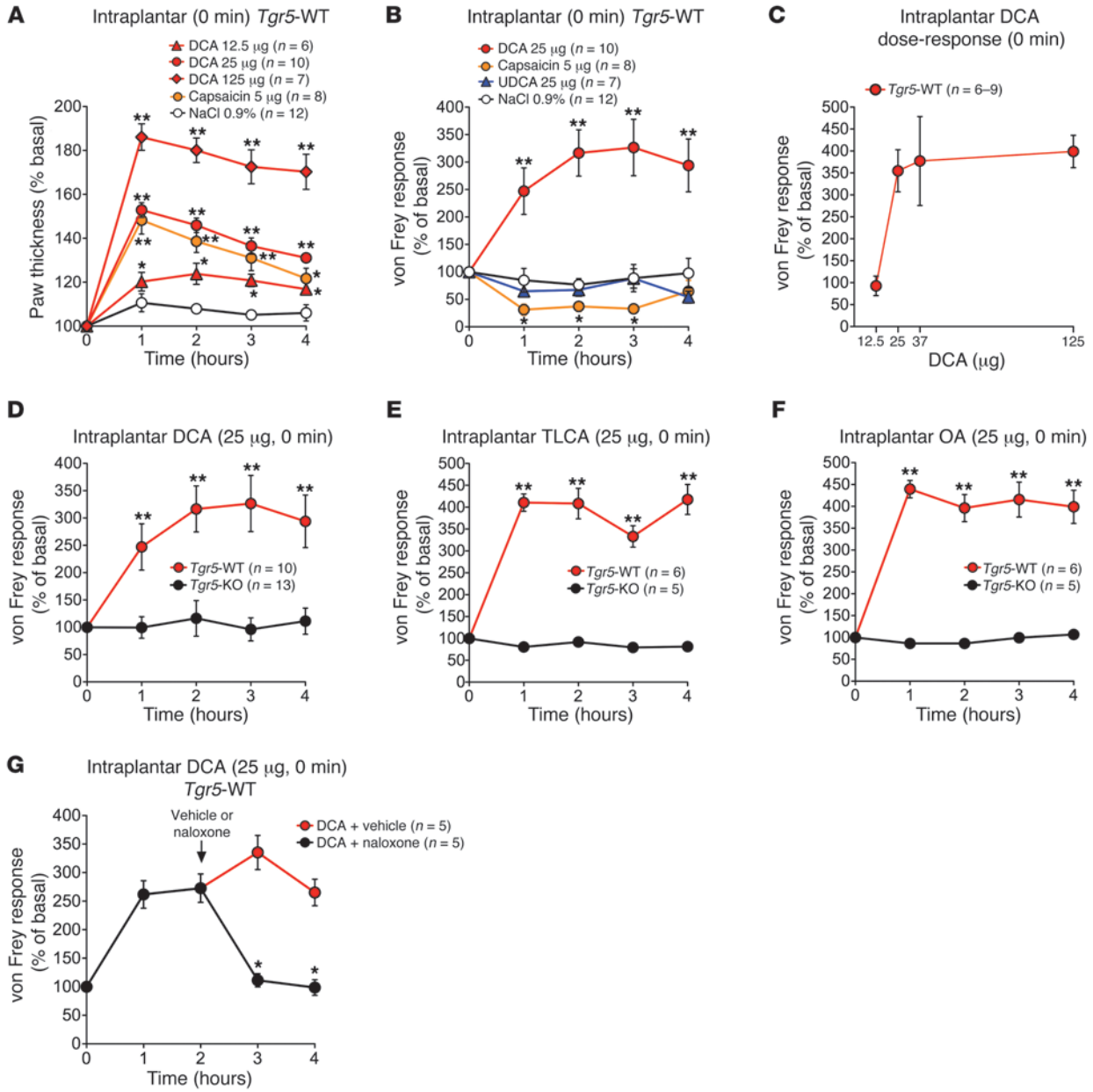

Figure 8

Peripheral mechanisms of BA- and TGR5-induced mechanical analgesia and edema in *Tgr5*-WT and *Tgr5*-KO mice. Test agents were injected into the plantar surface of the hind paw. Responses to stimulation of the plantar surface of the paw with von Frey filaments of graded stiffness and paw thickness were recorded. Results are expressed as percent basal value. An increased von Frey response indicates that a stiffer filament was required to induce withdrawal (mechanical analgesia), whereas a decreased response indicates that a less stiff filament was required to induce withdrawal (mechanical hyperalgesia). (**A**) Intraplantar injection of DCA (12.5–125 μg) or capsaicin (5 μg) increased paw thickness in *Tgr5*-WT mice, indicative of inflammatory edema. (**B**) Intraplantar DCA (25 μg), but not UDCA (25 μg), caused analgesia, whereas capsaicin (5 μg) caused hyperalgesia, in *Tgr5*-WT mice. (**C**) Intraplantar DCA (12.5, 25, 37.5, and 125 μg) stimulated dose-dependent analgesia measured at 3 hours in *Tgr5*-WT mice. (**D**) Intraplantar DCA (25 μg) caused analgesia in *Tgr5*-WT, but not *Tgr5*-KO, mice. (**E** and **F**) TLCA and OA (25 μg) caused analgesia in *Tgr5*-WT, but not *Tgr5*-KO, mice. (**G**) Naloxone or vehicle control was administered by intraplantar injection 2 hours after intraplantar injection of DCA (25 μg) to *Tgr5*-WT mice. Naloxone rapidly reversed the mechanical analgesia. $^{*}P < 0.05$, $^{**}P < 0.01$ vs. respective vehicle control (**A**, **B**, and **G**) or vs. *Tgr5*-KO (**D**, **E**, and **F**); ANOVA and Student-Newman-Keuls (**A** and **B**) or unpaired *t* test (**D**–**F**, and **G**). *n* is indicated.

related, with threshold response to 5 μg and maximal response to 25 μg (Figure 6E). Higher DCA doses caused severe scratching that damaged the skin, and were not further studied. Although TLCA and OA (25 μg) robustly stimulated scratching in *Tgr5*-WT mice, responses were markedly diminished in *Tgr5*-KO mice (Figure 6, F and G). Of all the tested BAs, OA stimulated the largest scratching response in *Tgr5*-WT mice (192.6 ± 15 events/30 minutes). UDCA (25 μg) had a small effect on scratching in *Tgr5*-WT

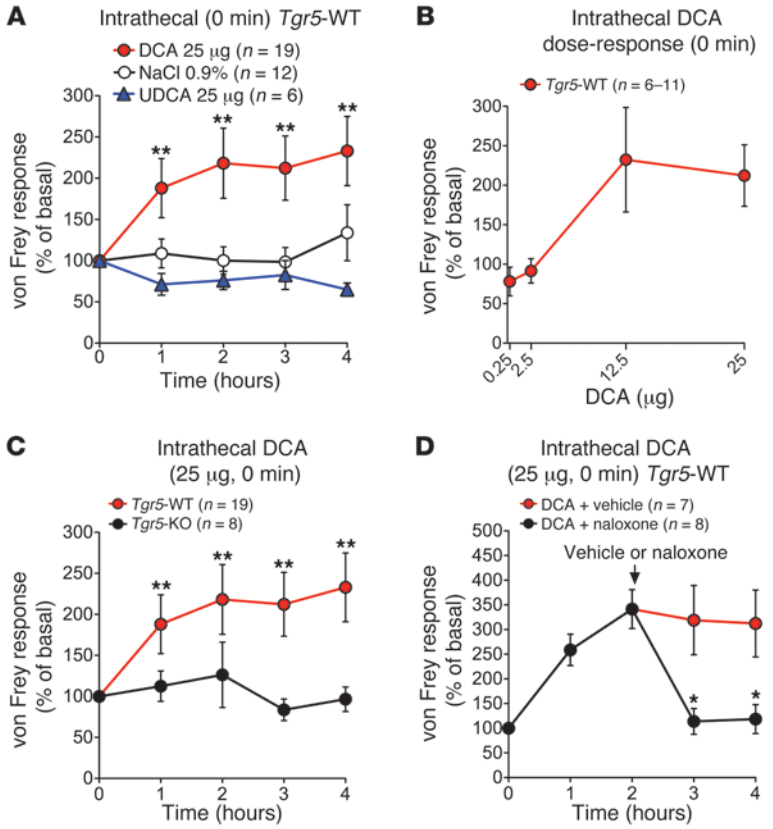

Figure 9
Central mechanisms of BA- and TGR5-induced mechanical analgesia in *Tgr5*-WT and *Tgr5*-KO mice. Test agents were injected intrathecally. Responses to stimulation of the plantar surface of the paw with von Frey filaments of graded stiffness were recorded. Results are expressed as percent basal value. (**A**) Intrathecal injection of DCA (25 μg), but not UDCA (25 μg), caused analgesia in *Tgr5*-WT mice. (**B**) Intrathecal DCA (0.25, 2.5, 12.5, and 25 μg) stimulated dose-dependent analgesia measured at 3 hours in *Tgr5*-WT mice. (**C**) Intrathecal DCA (25 μg) caused analgesia in *Tgr5*-WT, but not *Tgr5*-KO, mice. (**D**) Naloxone or vehicle control was administered systemically 2 hours after intrathecal injection of DCA (25 μg) to *Tgr5*-WT mice. Naloxone rapidly reversed the mechanical analgesia. **P* < 0.05 vs. respective vehicle control (**A** and **D**) or *Tgr5*-KO (**C**); ANOVA and Student-Newman-Keuls test (**A**) or unpaired *t* test (**C** and **D**). *n* is indicated.

mice that was similar in *Tgr5*-KO and *Tgr5*-Tg mice (Figure 6H). The established pruritogen histamine (50 μg) caused an equivalent degree of scratching in *Tgr5*-WT, *Tgr5*-KO, and *Tgr5*-Tg mice (Figure 6I). Figure 6J summarizes the scratching responses measured within 60 minutes of intradermal injection of vehicle (0.9% NaCl), DCA, TLCA, OA, UDCA, or histamine to *Tgr5*-WT, *Tgr5*-KO, and *Tgr5*-Tg mice. These data confirmed that TGR5 overexpression induced spontaneous scratching and that DCA, TLCA, and OA caused scratching that was highly dependent on TGR5 expression.

Deletion of GRPR or intrathecal administration of a GRPR antagonist suppresses scratching to diverse pruritogens (10). Compared with vehicle control, intrathecal injection of the GRPR antagonist [Tyr^4, D-Phe^{12}]-bombesin (53) caused an approximately 60% reduction in DCA-induced scratching in *Tgr5*-WT mice (102.0 ± 37.5 vs. 249.0 ± 89.6 events/60 minutes; $P = 0.001$; Figure 7A). These results indicate a major role for centrally released GRP in BA-evoked scratching.

Morphine, a MOR agonist, is a pruritogen, which implicates opioids as mediators of itch (12, 54). Systemic administration of the MOR antagonist naloxone, which crosses the blood-brain barrier, blunted the scratching response to DCA administered to *Tgr5*-WT mice 30 minutes after treatment (Figure 7B). A second challenge with DCA — administered 180 minutes after the first DCA injection, when naloxone was cleared — stimulated a 3.4-fold increase in scratching compared with the initial challenge (117.6 ± 20.0 vs. 34.9 ± 9.0 events/60 minutes; $P = 0.002$). Thus, opioids contributed to the pruritogenic actions of BAs.

Mediators such as histamine and tryptase that are released from mast cells when they degranulate are powerful stimulants of itching. To determine whether mast cells could contribute to BA-induced scratching, *Trg5*-WT mice were treated with the mast cell stabilizer and histamine H_1 receptor antagonist ketotifen or vehicle control (0.9% NaCl) prior to administration of DCA. DCA (25 μg) stimulated a similar degree of scratching in mice treated with ketotifen or vehicle (Figure 7C), which suggests that mast cells and histamine do not contribute to DCA-stimulated scratching.

Lysophosphatidic acid (LPA) has been identified in the serum of cholestatic patients as a potential pruritogen; when administered to mice, LPA induces scratching (55, 56). To assess whether TGR5 could contribute to LPA-evoked itch, scratching was examined in *Tgr5*-WT and *Tgr5*-KO mice. Intradermal injection of LPA (100 μg) stimulated a similar degree of scratching in *Tgr5*-WT and *Tgr5*-KO mice (Figure 7D). To determine whether LPA can activate TGR5, HEK293 cells expressing human TGR5 were incubated with LPA or DCA. cAMP formation was measured as an index of receptor activation, since TGR5 couples to Gαs (28, 29). DCA stimulated cAMP generation in HEK293 cells with an EC_{50} of 99.6 ± 13.3 μM; in contrast, LPA up to 500 μM did not affect cAMP levels (Figure 7E). Thus, TGR5 did not mediate the pruritogenic effects of LPA, and LPA did not directly activate TGR5.

To determine whether BAs can act centrally to cause itch, DCA (25 μg, 5 μl) or vehicle (0.9% NaCl, 5 μl) was injected intrathecally to *Tgr5*-WT mice, and scratching behavior was recorded. There was no difference in the frequency of scratching events between DCA- and vehicle-treated mice within 30 minutes of injection (vehicle, 3.8 ± 0.5 events/30 minutes; DCA, 4.8 ± 1.0 events/30 minutes; $n = 4$). Thus, DCA stimulated scratching when administered peripherally, but not centrally. These results indicated that BAs and

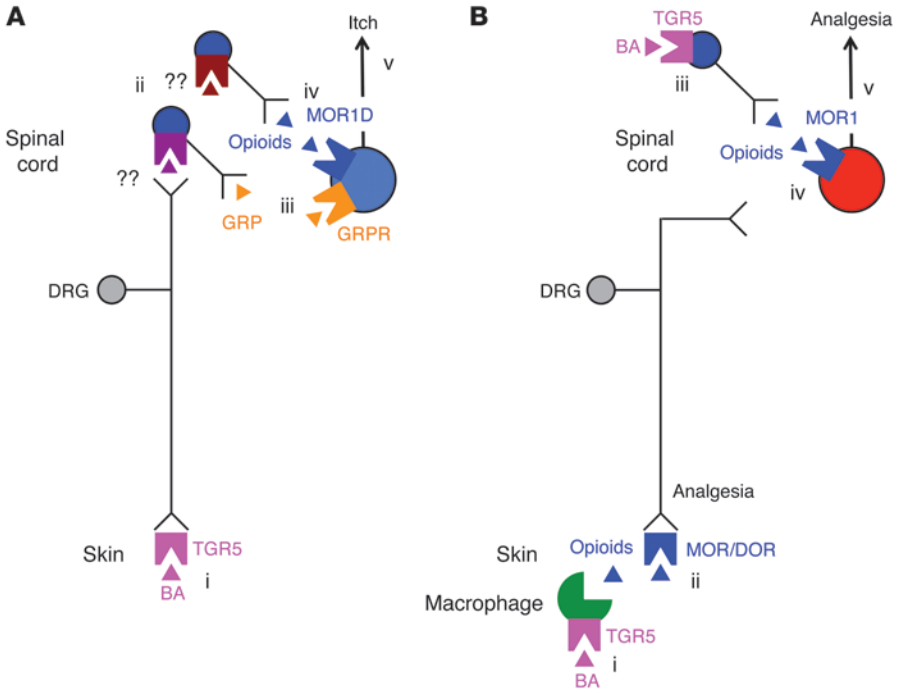

Figure 10

Hypothesized mechanisms of BA- and TGR5-induced itch and analgesia. (**A**) Mechanisms of itch. BAs in the skin activate TGR5 on sensory nerve endings (i), which increases neuronal excitability and stimulates release of unknown transmitters from the central projections of sensory nerves in dorsal horn of the spinal cord (ii). The transmitters induce release of GRP (iii) and opioids (iv) from spinal neurons. GRP activates GRPR and opioids activate the MOR1D/GRPR heterodimer on itch-selective spinal neurons. Activated GRPR induces itch (v). (**B**) Mechanisms of analgesia. BAs in the skin activate TGR5 on dermal macrophages (i) to stimulate release of opioids that activate MORs and δ-opioid receptors (DOR) on sensory nerve endings to induce peripheral mechanisms of analgesia (ii). BAs in the spinal cord activate TGR5 on spinal neurons (iii) to stimulate release of opioids that activate MOR1 on pain-selective spinal neurons (iv). Activated MOR1 induces central mechanisms of analgesia (v).

a TGR5-selective agonist robustly stimulated scratching behavior in mice by activating TGR5 in the periphery. We therefore conclude that TGR5-induced pruritus is mediated by central action of GRP and also requires opioids, but is independent of mast cells.

BAs activate TGR5 and cause opioid-mediated mechanical analgesia. Bile duct resection in mice, which mimics cholestatic disease, induces an analgesia to mechanical stimulation of the paw by an opioid-dependent mechanism (5). To evaluate whether exogenous BAs can mimic the effects of bile duct ligation and cause analgesia, BAs were administered to mice by intraplantar injection. Paw thickness was measured to assess inflammatory edema, and paw withdrawal responsiveness to stimulation of the plantar surface with graded von Frey filaments was examined to assess mechanical pain.

After intraplantar injection to *Tgr5*-WT mice, DCA (12.5–125 μg) caused a large and dose-dependent increase in paw thickness that was maximal at 1 hour and sustained for at least 4 hours (Figure 8A), indicative of edema. Capsaicin (5 μg) also induced edema. After intraplantar injection of DCA (25 μg) to *Tgr5*-WT mice, the filament stiffness required to elicit paw withdrawal increased, indicative of mechanical analgesia. The increased von Frey score was detected within 1 hour and maintained for at least 4 hours, with a maximal effect at 2–3 hours (Figure 8B). Intraplantar injection of UDCA (25 μg) or vehicle (0.9% NaCl) had no effect on von Frey score. Conversely, after intraplantar injection of capsaicin to *Tgr5*-WT mice, the filament stiffness required to elicit paw withdrawal decreased (Figure 8B), indicative of mechanical hyperalgesia. At 2 hours after intraplantar injection, the von Frey responses were 316.6% ± 44.4% of basal for DCA, 67.6% ± 12.3% for UDCA, 76.6% ± 11.5% for vehicle, and 37.2% ± 14.1% for capsaicin (P = 0.002, DCA vs. vehicle). The analgesic action of intraplantar DCA was dose related, with a maximal effect observed with 37.5 μg (Figure 8C). In marked contrast to the analgesia observed in *Tgr5*-WT mice, intraplantar DCA did not cause mechanical analgesia in *Tgr5*-KO mice (Figure 8D). Similar to DCA, intraplantar injection of TLCA or OA (25 μg) caused mechanical analgesia in *Tgr5*-WT, but not *Tgr5*-KO, mice (Figure 8, E and F).

To determine whether opioids released locally within the paw contribute to BA-induced analgesia, DCA was administered by intraplantar injection to *Tgr5*-WT mice; 2 hours later, mice received intraplantar injection of naloxone or vehicle. In vehicle-treated mice, DCA induced mechanical analgesia that was sustained for at least 4 hours (Figure 8G). Naloxone fully reversed this analgesia within 1 hour.

In order to investigate whether BAs can affect pain by central mechanisms, BAs were injected intrathecally, and withdrawal responses to mechanical stimulation of the plantar surface of the paw with von Frey filaments was assessed. In *Tgr5*-WT mice, intrathecal DCA (25 μg) caused mechanical analgesia within 1 hour that was maintained for at least 4 hours, with a maximal effect at 2 hours (Figure 9A). Intrathecal injection of UDCA (25 μg) or vehicle (0.9% NaCl) had no effect. At 2 hours after intrathecal injection, responses were 218.3% ± 43.7% of basal for DCA, 76.1% ± 12.1% for UDCA, and 100.2% ± 17.4% for vehicle (P = 0.002, DCA vs. vehicle). DCA-induced analgesia was dose related, with a maximal response detected with 12.5 μg (Figure 9B). In contrast, intrathecal DCA did not cause mechanical analgesia in *Tgr5*-KO mice (Figure 9C). TGR5 overexpression did not influence the degree of analgesia in *Tgr5*-WT mice (data not shown), which was presumably maximal.

To evaluate the contribution of endogenous opioids to BA-induced analgesia, DCA (25 μg) was administered intrathecally to *Tgr5*-WT mice, and after 2 hours, mice received naloxone or vehicle systemically. In vehicle-treated mice, DCA induced mechanical analgesia that was sustained for at least 4 hours (Figure 9D). Naloxone fully reversed this analgesia within 1 hour.

These results indicated that BAs and TGR5-selective agonists induced mechanical analgesia by activating TGR5 in the periphery and spinal cord. TGR5-induced mechanical analgesia was mediated by opioids. Although intraplantar injection of BAs caused

inflammatory edema, the inflammation was unrelated to the analgesia: both DCA and capsaicin caused edema, yet DCA induced analgesia, whereas capsaicin had the opposite effect.

Discussion

We here report a new mechanism by which BAs cause itch and analgesia: TGR5 is expressed by sensory neurons that transmit itch and pain, and TGR5 activation enhances neuronal excitability. BAs stimulate release of GRP and Leu-ENK, modulators of itch and pain, from spinal cord with attached DRG. Additionally, BAs cause GRP- and MOR-dependent scratching and MOR-dependent antinociception. Our major finding was that BA-induced pruritogenic and analgesic responses were abrogated or absent in mice with loss of TGR5 function, whereas scratching was exacerbated in mice with gain of TGR5 function. These findings may provide insight into the mechanisms of cholestatic pruritus (2) and painless jaundice (3, 4). TGR5 antagonists may represent a new treatment for cholestatic pruritus, whereas TGR5 agonists may be analgesics.

Our results showed that BAs can signal to sensory neurons and cause TGR5- and GRP-mediated itch (Figure 10A). Using single-cell RT-PCR, we detected *Tgr5* mRNA in 36% of small-diameter DRG neurons, where *Tgr5* was often coexpressed with other mediators of itch, including *Grp* (10, 42) and the *Trpa1* and *Trpv1* ion channels (14, 43, 44). Using a TGR5-selective antibody, we found TGR5-IR to be localized to 28% of all DRG neurons and more than 60% of peptidergic neurons. In accord with a prior report (50), GRP-IR was expressed at low levels, which precluded quantification of the extent of colocalization with TGR5-IR. However, our results support other reports of *Grp* mRNA and GRP-IR in small-diameter DRG neurons expressing CGRP, SP, and TRP channels (10, 42).

Our electrophysiological studies of isolated DRG neurons provided evidence that BAs can induce neuronal hyperexcitability by activating TGR5. We observed that brief exposure of DRG neurons to the BAs DCA and TLCA, which potently activate TGR5 (28, 29), caused decreased rheobase and increased AP discharge frequency at 2× rheobase, indicative of increased intrinsic excitability of these neurons. Several observations suggest that these effects are mediated by activation of TGR5. First, DCA did not affect the excitability of DRG neurons from *Tgr5*-KO mice. Second, OA — a potent TGR5 agonist that does not activate nuclear BA receptors (48) — was the strongest stimulant of excitability. Third, UDCA — which does not activate TGR5 or is a weak agonist (28, 49), yet retains the irritant and detergent properties of BAs — had no effect on neuronal excitability at any concentration tested. The effects of DCA, TLCA, and OA on rheobase were concentration dependent, and, with the exception of TLCA, all agonists increased AP discharge frequency at the highest tested concentrations. Importantly, BAs increased neuronal excitability at concentrations similar to those in the circulation and skin of cholestatic patients (18, 19). Collectively, our data indicate that BAs and a TGR5 agonist can directly regulate the excitability of small-diameter DRG neurons. Although our results support the hypothesis that BAs increase the intrinsic excitability of DRG neurons by activating TGR5, we cannot exclude the possibility that BAs also regulate excitability by other mechanisms (which may include activating nuclear BA receptors), or through effects on other cell surface receptors or ion channels. Further studies are required to investigate these possibilities. We recorded from all small-diameter DRG neurons, even though only a portion of these neurons (36%) expressed *Tgr5* mRNA. Thus, the magnitude of the effects of BAs on TGR5-expressing neurons is likely to be substantially greater than the average effects we observed when recording from all neurons, regardless of *Tgr5* expression. Differences in the level of *Tgr5* expression between neurons could also account for the variability of effects of BAs on neuronal excitability. Although DCA and TLCA did not induce the spontaneous firing of APs in DRG neurons, OA did induce AP discharge in 35% of small-diameter neurons, in accord with the proportion of neurons expressing *Tgr5* mRNA. Our results raise the possibility that BAs in peripheral tissues could activate TGR5 on nerve endings, leading to AP discharge and central transmission. The limitations of our study are that we applied agonists to the neuronal soma rather than the nerve endings and that we made recordings from isolated neurons in culture, where DRG soma have no stimulatory inputs beyond the depolarizing currents injected as part of the experimental protocol. Further studies are required to determine whether application of BAs to the skin results in central transmission. Although we detected TGR5-IR in the soma of DRG neurons, we did not detect TGR5-IR in nerve fibers in the skin or the dorsal horn, which is a caveat of our interpretation. Our inability to detect TGR5 in nerve fibers is likely related to the low density of innervation by TGR5-positive nerves and inadequate sensitivity for detecting the low receptor levels in nerve fibers, since we are also unable to detect TGR5 in the fibers of enteric neurons that highly express TGR5 in the soma (39).

We found that TGR5 activation stimulated the release of neuropeptides from segments of rat spinal cord with attached dorsal roots. DCA, TLCA, and OA stimulated a concentration-dependent release of GRP-IR that required the presence of extracellular calcium ions, whereas UDCA had minor stimulatory action only at the highest tested concentration. We were unable to study BA-evoked neuropeptide release from *Tgr5*-WT or *Tgr5*-KO mice because larger amounts of tissues were required for these analyses, which we obtained from rats. Thus, although our results suggest that BAs stimulate neuropeptide release by a TGR5-mediated mechanism, further studies using selective antagonists are required to definitively determine the involvement of TGR5. The GRP released from this preparation could derive from the central projections of DRG neurons or from spinal neurons. Although GRP has been detected in DRG neurons (10, 42), GRP is more prominently expressed by spinal neurons, including those within laminae I and II of the dorsal horn (50). We detected GRP-IR in both locations. However, 2 observations suggested that BAs release GRP from intrinsic spinal neurons rather than from the terminals of DRG neurons in the dorsal horn. First, preincubation of tissues with the TRPV1 agonist capsaicin, which depletes neuropeptides from nociceptors, did not prevent BA-evoked GRP-IR release. Second, capsaicin did not directly stimulate GRP-IR release. In marked contrast, capsaicin pretreatment prevented BA-stimulated release of CGRP-IR, and capsaicin directly stimulated CGRP-IR secretion. Thus, whereas CGRP derives from TRPV1-expressing DRG neurons, GRP probably derives from spinal neurons that do not express TRPV1. Further studies are require to determine the mechanism by which BAs induce GRP release from spinal neurons. One possibility is that BAs excite DRG neurons, which stimulate the release of a transmitter within the dorsal horn that promotes the secretion of GRP from spinal neurons. This possibility is in line with the ability of BAs to induce hyperexcitability of DRG neurons. The spinal transmitter that is released by BAs remains to be identified, although glutamate has been proposed as a transmitter for GRP-dependent and -independent synaptic transmission of itch within the dorsal

horn (57). We cannot exclude the possibility that SP and CGRP also contribute to BA-evoked itch, since both peptides colocalized with TGR5 in DRG neurons, and TGR5 agonists stimulated CGRP release from spinal cord/DRG. Further studies are required to assess the contributions of SP and CGRP to BA-stimulated itch. Our suggestion that BAs evoke GRP release from spinal rather than DRG neurons raise questions about the function of GRP in DRG neurons. The possibility that other pruritogens stimulate GRP release from DRG neurons remains to be investigated.

Our results showed that BAs cause scratching behavior by TGR5- and GRPR-mediated mechanisms. Intradermal injection of DCA, TLCA, and OA caused a robust concentration-dependent increase in scratching, whereas central administration of DCA had no effect. These results indicate that BAs cause scratching by activating TGR5 in the periphery, but not in the spinal cord. Antagonism of spinal GRPRs reduced BA-induced scratching, consistent with stimulation of an itch-selective pathway involving GRP release and activation of the GRPR on itch-selective neurons in the dorsal horn (10, 11). The pruritogenic effects of DCA, TLCA, and OA depended on the level of *Tgr5* expression. *Tgr5* deletion inhibited DCA-, TLCA-, and OA-stimulated scratching, whereas DCA-evoked scratching was more frequent in mice overexpressing *Tgr5*. However, histamine-stimulated scratching was unaffected by the level of *Tgr5* expression. Thus, we conclude that TGR5 selectively mediates BA-induced itch. In contrast to the analgesic effects of BAs, which were absent from *Tgr5*-KO mice, BA-stimulated scratching was not abolished by *Tgr5* deletion, and UDCA also caused a low level of TGR5-independent scratching. Thus, we cannot exclude the possibility that BAs regulate sensory neurons by additional mechanisms, or that BAs activate TGR5 on other cells in the skin that release pruritogens. Studies using antagonists of plasma membrane and nuclear BA receptors and of mice selectively lacking neuronal TGR5 will be required to examine these possibilities. However, administration of a mast cell stabilizer and H_1 receptor antagonist did not affect DCA-evoked scratching, which excludes involvement of mast cells and histamine in this process.

The level of *Tgr5* expression per se determined scratching behavior, regardless of increased levels of BAs, since mice with a gain of *Tgr5* function exhibited a 3.4-fold increase in spontaneous scratching compared with *Tgr5*-WT mice and a 7-fold increase in scratching compared with *Tgr5*-KO mice. Nothing is known about the level of *TGR5* expression in cholestatic patients, although we detected increased TGR5-IR in neurons of mice after bile duct ligation (N.W. Bunnett and C.U. Corvera, unpublished observations). Thus, increased expression of TGR5 in sensory neurons may amplify responsiveness to physiological levels of BAs, which fluctuate with episodic secretion of bile (58).

We detected TGR5 in small-diameter DRG neurons that also expressed TRPV1 and TRPA1, although the role of these channels in BA- and TGR5-mediated itch is unknown. TRPV1 contributes to the pruritogenic actions of histamine (43), and GPCRs for some pruritogens activate TRPA1, which mediates their pruritogenic effects (44). Further studies are required to determine whether TGR5 couples to TRP channels that mediate itch transmission.

We conclude that BAs induce analgesia by TGR5- and opioid-dependent mechanisms (Figure 10B). Intraplantar injection of DCA, TLCA, and OA and intrathecal injection of DCA reduced paw responsiveness to von Frey stimulation, indicative of mechanical analgesia by peripheral and central mechanisms. UDCA had no effect, and DCA, TLCA, and OA responses were absent from *Tgr5*-KO mice, and thus require TGR5 expression. Intraplantar DCA also caused edema, possibly due to release of SP and CGRP from cutaneous sensory nerves. However, the edema was unrelated to the analgesic actions of BAs, since capsaicin caused a similar degree of inflammation, yet was hyperalgesic. Naloxone reversed analgesia that was induced by peripherally and centrally administered DCA, implicating opioids and MOR. Mice with cholestasis also exhibit opioid-dependent antinociception (5). The source of opioids released after peripheral and central administration of DCA is unknown. We found TGR5-IR to be localized to dermal macrophages, consistent with other reports (28, 37). Leukocytes, including macrophages, express opioids that can activate MORs and δ-opioid receptors on the peripheral terminals of DRG neurons to suppress nociception (46). Further studies are required to determine whether BAs activate TGR5 on dermal macrophages to release opioids that activate receptors on sensory nerves in the skin and cause antinociception. However, the observation that intraplantar naloxone reversed analgesia to intraplantar DCA supports the local release of opioids, possibly from macrophages. We also detected TGR5-IR in regions of the spinal cord known to express opioids, including laminae I, II, and X (51), and TGR5 agonists stimulated release of Leu-ENK–IR from spinal cord. As expected, BA-evoked release of Leu-ENK–IR was unaffected by preincubation with capsaicin, and thus derives from spinal neurons. Our results suggest that BAs may activate TGR5 on spinal neurons to release opioids that induce analgesia. Further studies are required to identify the subtypes of spinal neurons that express TGR5 and to determine whether TGR5 is expressed by neurons that release opioids. It is not known whether cholestasis leads to increased levels of BAs in the spinal cord. However, BAs have been detected in rat brain (59) and in cerebrospinal fluid of normal human subjects (60), and levels are increased in patients with liver failure (61).

Opioids are pruritogens, and itch is a limiting side effect of intrathecal opiate analgesics (8). Naloxone inhibited DCA-induced scratching, implicating MOR in the central transmission of BA-induced itch (Figure 10A). Our observation that peripheral (but not central) BAs caused opioid-dependent itch suggests that BAs in the periphery can stimulate the central release of opioids. However, the mechanisms of this release remain to be determined. MOR isoforms that are selectively expressed by itch- or pain-transmitting spinal neurons may mediate the pruritogenic and analgesic actions of spinal opioids (12). Interaction between the MOR1D isoform and GRPR in itch-transmitting spinal neurons provides a mechanism for morphine to activate GRPR and induce itch, whereas morphine activation of MOR1 in pain-transmitting spinal neurons mediates antinociception.

Our observations provide insight into the itch and analgesia that can accompany liver disease. The findings that BA levels are elevated in serum and skin of cholestatic patients (18, 19), that BAs cause itch (20, 21), and that BA-binding resins are an effective treatment (22) implicate BAs as causative agents of cholestatic itch. We observed hyperexcitability of DRG neurons and release of transmitters of itch and analgesia at BA concentrations, in line with the elevated levels of total BAs detected in serum of patients with cholestatic disease (61). However, BA levels do not necessarily correlate with pruritus severity (2, 22, 56, 62), and other pruritogens may also mediate itch. Of these, LPA is a strong candidate (55, 56). The levels of LPA and autotaxin, an enzyme that generates LPA, are elevated in the circulation of cholestatic patients with pruritus, and autotaxin levels correlate with the intensity of

itch (56). Moreover, LPA stimulates scratching behavior in mice (55, 56). Our results showed that LPA did not activate TGR5, even at concentrations far in excess of those that activate LPA receptors (i.e., 500 μM), and that TGR5 did not mediate LPA-evoked scratching. Moreover, in contrast to BA-evoked itch, ketotifen inhibits LPA-evoked itch (55), suggesting different mechanisms. However, we cannot exclude the possibility that LPA mediates cholestatic itch. Although the contribution of GRP to cholestatic pruritus has not been investigated, opioids have been implicated, since naloxone alleviates cholestatic pruritus (26) and analgesia (5), and circulating opioids increase during cholestasis, although levels do not necessarily correlate with the degree of itch (23, 24, 56). Additional studies are required to examine whether centrally and peripherally released opioids contribute to BA-evoked itch and analgesia and to investigate the involvement of TGR5 in itch in patients with cholestatic disease.

Our results raise questions about the role of TGR5 in the nervous system. Although TGR5 may allow primary spinal afferent and spinal neurons to respond to elevated BA levels during cholestatic diseases, what is the physiologically relevant activator of neuronal TGR5? One possibility is that TGR5 allows sensory nerves to detect and respond to the increased circulating levels of BAs after feeding (58) or to detect BAs that are synthesized in the central nervous system (60). Alternatively, there may be distinct TGR5 agonists in the nervous system, such as neurosteroids that are structurally related to BAs and are potential TGR5 agonists in the central nervous system (40, 41). The physiological relevance of these new sensory mechanisms remains to be determined.

Methods

Animals. *Tgr5*-KO, *Tgr5*-Tg and *Tgr5*-WT mice (C57BL/6 background) have been described previously (32). Mice were maintained as heterozygotes, and age- and gender-matched littermates were studied. C57BL/6 mice and Sprague-Dawley rats were from Charles River Laboratories and Harlan Laboratories. Animals were maintained in a temperature-controlled environment with a 12-hour light/12-hour dark cycle and free access to food and water. Animals were killed by anesthetic overdose and bilateral thoracotomy.

Dissociation and selection of DRG neurons. Male and female C57BL/6 mice were transcardially perfused with Krebs bicarbonate solution (118 mM NaCl, 5.4 mM KCl, 1.0 mM NaH_2PO_4, 1.2 mM $MgSO_4$, 1.9 mM $CaCl_2$, 25.0 mM $NaHCO_3$, 11.1 mM dextrose, 95% O_2, and 5% CO_2 [pH 7.4]). DRG were removed, pooled, and incubated in Ca^{2+}-, Mg^{2+}-free Hanks balanced salt solution containing collagenase and dispase II (both 2 mg/ml; Sigma-Aldrich) for 30 minutes at 37°C. Neurons were dissociated by trituration with a fire-polished Pasteur pipette, followed by 2 repeated enzymatic digestions for 20 minutes at 37°C. Neurons were washed by centrifugation and resuspension (3×, 1,000 *g*, 2 minutes) and suspended in DMEM medium containing 10% FBS. Dissociated neurons were plated onto coverslips coated in 0.1 mg/ml poly-D-lysine and 0.004 mg/ml laminin, then incubated in DMEM containing 10% FBS in a humidified incubator (37°C, 95% air, 5% CO_2) until selection for single-cell RT-PCR within 8 hours of DRG removal. Cover slips were perfused with Krebs solution (95% O_2, 5% CO_2). Individual small-diameter neurons (<25 μm) were drawn into a glass pipette (tip diameter, 25–100 μm) pulled with a micropipette puller (model P-87; Sutter Instruments Co.) by applying negative pressure (63). The pipette tip was broken into a PCR tube containing 1 μl resuspension buffer and RNAse inhibitor (RNAseOUT, 2 U/μl; Invitrogen). The tubes were immediately snap frozen.

Single-cell RT-PCR. Single neurons were processed to obtain cDNA using Superscript III Cells Direct cDNA Synthesis Kit (Invitrogen) according to the manufacturer's instructions. Water was added to one-third of the sample for the negative RT control. The remainder of the sample was reverse transcribed using Superscript III Reverse Transcriptase. PCR reactions used the following intron-spanning mouse primers: *Tgr5* outer forward, 5′-CACTGCCCTTCTCTCTGTCC-3′; *Tgr5* outer reverse, 5′-TCAAGTCCAGGTCAATGCTG-3′; *Tgr5* inner forward, 5′-TGCTCTTCTTGCTGTGTTGG-3′; *Tgr5* inner reverse, 5′-GTCCCTCTTGGCTCTTCCTC-3′; *Grp* outer forward, 5′-CACGGTCCTGGCTAAGATGT-3′; *Grp* outer reverse, 5′-GGGTTTTGTTTTGCTCCTTG-3′; *Grp* inner forward, 5′-GGCTGTGGGACACTTAATGG-3′; *Grp* inner reverse, 5′-CCCAAGTAGGCTGGAGACTG-3′; *Trpv1* forward, 5′-TCACCGTCAGCTCTGTTGTC-3′; *Trpv1* reverse, 5′-GGGTCTTTGAACTCGCTGTC-3′; *Trpa1* forward, 5′-GGAGCAGACATCAACAGCAC-3′; *Trpa1* reverse, 5′-GCAGGGGCGACTTCTTATC-3′; *Actb* forward, 5′-CTGGTCGTCGACAACGGCTCC-3′; *Actb* reverse, 5′-GCCAGATCTTCTCCATG-3′ (Invitrogen). The PCR reaction contained primers, 0.5 U HotStar Taq Polymerase, 2.5 mM $MgCl_2$, 10 mM dNTP, and 10× PCR buffer (Qiagen) (20 μl final volume). PCR reaction conditions were 50 cycles of initial activation at 95°C for 15 minutes, denaturation at 94°C for 30 seconds, annealing at 60°C for 30 seconds, extension at 72°C for 1 minute, and final extension at 72°C for 10 minutes. As a positive control, RNA was isolated from whole DRG, spinal cord, or gall bladder and was reverse transcribed using Omniscript RT Kit (Qiagen). As negative controls, fluid from the vicinity of the collected cells was amplified, or RT was omitted. Products were separated by electrophoresis (2% agarose), stained using ethidium bromide, and sequenced to confirm identity.

Immunolocalization and microscopy. DRG and spinal cord (thoracic, lumbar, and sacral) from C57BL/6 mice (male and female, 6–8 weeks of age) and Sprague-Dawley rats (male, 200 g) were collected and fixed (4% paraformaldehyde, 100 mM PBS, pH 7.4) for 2 hours on ice. Tissues were cleared in PBS (3×, 10 minutes), incubated in sucrose (30% w/v in PBS, overnight, 4°C), and embedded in OCT (Sakura Finetek). Frozen sections (12 μm) were collected onto glass slides and air dried (1 hour, room temperature). Sections were blocked (10% normal horse serum, 0.1% Triton X-100 in PBS, 1 hour, room temperature), then incubated with the following primary antibodies in blocking buffer (overnight, 4°C): rabbit anti-TGR5 (1:200–1:500, P87/88; ref. 39); sheep anti-CGRP (1:1,000; ref. 64); rat anti-SP (1:800; ref. 65); goat anti-GRP (1:100, C-20; Santa Cruz Biotechnology); rabbit anti-$GRP^{17–27}$ (1:1,000, 1078; ref. 45); human anti-Hu (pan-neuronal marker, 1:10,000; ref. 66); or IB4-FITC (1:400; Vector Laboratories). Sections were washed (3× PBS, 10 minutes) and incubated for 1 hour at room temperature with the following fluorescent secondary antibodies: donkey anti-sheep IgG–Alexa Fluor 488 (1:500), anti-sheep IgG–Alexa Fluor 647 (1:500), anti-rabbit IgG–Alexa Fluor 488 (1:1,000), anti-rabbit IgG–Alexa Fluor 594 (1:500; Molecular Probes), anti-human IgG–Texas Red (1:100), or anti-rat IgG–FITC (1:100; Jackson ImmunoResearch). Tissues were washed and mounted using Prolong Gold (Invitrogen). Specificity of the TGR5 antibody was determined by incubation of the TGR5 antibody with DRG from *Tgr5*-WT or *Tgr5*-KO mice, or by preadsorption of diluted TGR5 antibody with receptor fragment that was used for immunization (GPSIAYHPSSQSSVDLDLN, 50 μM, overnight, 4°C) prior to staining. Specificity of the secondary antibodies was evaluated by replacement of the primary TGR5 antibody with normal rabbit IgG (1:500, SC-2027; Santa Cruz Biotechnology) or by omission of the primary antibody. Positive and negative control samples were imaged under identical conditions. Specificity of the 2 GRP antibodies was determined by simultaneous staining of DRG sections and of sections and myenteric plexus whole-mounts of the gastric antrum (39), an established site of GRP expression that served as a positive control.

To localize TGR5 in the skin, frozen sections (6 μm) of mouse skin were prepared, and TGR5 was detected by immunohistochemistry using rabbit

anti-TGR5 (1:1,000, P87/88; ref. 39) and the Biotin-Avidin System (Vector Laboratories). Sections were counterstained with hematoxylin.

Slides were examined by confocal microscopy using a Zeiss LSM510 Meta microscope, or by bright field microscopy using a Zeiss Axioplan microscope, with ×10 Plan Apochromat (NA 0.45) and ×20 Plan Neofluar (NA 0.5) objectives (Carl Zeiss Inc.). Image brightness and contrast were modified using Adobe Photoshop CS5. Images of TGR5-positive and -negative control slides were collected and processed identically.

Coexpression of TGR5-IR with neurochemical markers in DRG neurons was evaluated by examination of captured images (single plane); only those neurons with a clearly defined nucleus were included in counts. All positive neurons from each image were counted. The proportion of TGR5-positive neurons was expressed as a percentage of neurochemically defined neurons and of the total number of neurons. The cross-sectional area of TGR5-positive DRG neurons was determined from captured images using ImageJ software (NIH). Only neurons with a detectable nucleus were considered in this analysis, and only every third section was analyzed to avoid duplication of measurements. Bins of 50 μm^2 were used to subdivide neurons based on size.

Patch-clamp recordings. DRG (thoracic and lumbar) from mice (C57BL/6 *Tgr5*-WT and *Tgr5*-KO, male) were acutely dissociated (47). Briefly, DRG were incubated in collagenase (1 mg/ml; Worthington) and dispase (4 mg/ml; Roche) for 10 minutes at 37°C, triturated with a fire-polished Pasteur pipette, and incubated for an additional 5 minutes at 37°C. Dissociated neurons were plated onto vitrogen-coated coverslips and stored in a humidified incubator (37°C, 95% air, 5% CO_2) until retrieval (4–24 hours) for electrophysiological studies. Perforated patch-clamp recordings were made from small-diameter neurons (<30 pF capacitance) in current clamp mode at room temperature (47). The pipette solution contained 110 mM K-gluconate, 30 mM KCl, 10 mM HEPES, 1 mM $MgCl_2$, and 2 mM $CaCl_2$; the external solution contained 140 mM NaCl, 5 mM KCl, 10 mM HEPES, 10 mM glucose, 1 mM $MgCl_2$, and 2 mM $CaCl_2$ (pH 7.25). The recording chamber was continuously perfused with external solution, and agonists were applied using a multi-barrel fast-flow system. The resting membrane potential, input resistance, rheobase (current required to generate 1 AP), and AP discharge frequency at 2× rheobase were recorded. Input currents were applied for 500 ms. Recordings were made from the same neurons under control basal conditions or after exposure to DCA, TLCA, UDCA, or OA (10, 30, or 100 μM) or vehicle (1% DMSO, 0.9% NaCl) for 10 minutes.

Neuropeptide release. Slices (0.4 mm) of spinal cord with attached dorsal roots from male Sprague-Dawley rats (combined cervical, thoracic, and lumbar-sacral segments) were prepared at 4°C (McIlwain Tissue Chopper). Slices (100 mg) were superfused with Krebs solution (119 mM NaCl, 25 mM $NaHCO_3$, 1.2 mM KH_2PO_4, 1.5 mM $MgSO_4$, 2.5 mM $CaCl_2$, 4.7 mM KCl, 11 mM D-glucose, 95% CO_2, 5% O_2, 37°C) containing 0.1% BSA and peptidase inhibitors (1 μM phosphoramidon and 1 μM captopril) (67). Tissues were stabilized for 90 minutes, after which superfusate was sampled at 10-minute intervals. After collection of 2 basal samples, slices were stimulated with DCA, TLCA, UDCA, or OA (10–500 μM) for 60 minutes. At the end of the experiment, tissues were blotted and weighed. Fractions (2 ml) were freeze-dried and reconstituted with assay buffer, and GRP-IR, Leu-ENK–IR, and CGRP-IR were determined by enzyme immunoassays (Phoenix Pharmaceutical). Peptide concentrations were calculated as picomoles per gram tissue wet weight. To examine whether BA-evoked neuropeptide release required calcium, slices were perfused with calcium-free Krebs (1 mM EDTA). To determine whether neuropeptides were released from primary spinal afferent expressing TRPV1, either tissues were preincubated with capsaicin (10 μM, 20 minutes) before stimulation with BAs, or the direct stimulatory effects of capsaicin (0.1 μM) on neuropeptide release were examined.

Scratching behavior. *Tgr5*-WT, *Tgr5*-KO, and *Tgr5*-Tg mice were studied (male and female, 6–20 weeks of age). The fur at the base of the neck was shaved, and mice were placed in individual cylinders on a glass shelf. Mice were acclimatized to the experimental room, restraint apparatus, and investigator for 2-hour periods on 2 successive days before experiments. Peripheral administration of test agents — DCA, TLCA, OA, or UDCA (5–25 μg); histamine (50 μg); or vehicle (0.9% NaCl, 10 μl) — was done by intradermal injection at the nape of the neck. For central administration, DCA (25 μg) or vehicle (0.9% NaCl, 5 μl) were injected intrathecally (L4/L5) in conscious mice. Hind limb scratching of the injection site was video recorded for 240 minutes. To examine the contribution of GRP, the GRPR antagonist [Tyr^4, $D\text{-}Phe^{12}$]-bombesin (2 mM, 16 μg; AnaSpec; ref. 53) or vehicle (0.9% NaCl, 5 μl) was injected intrathecally (L4/L5) 10 minutes before DCA injection. To evaluate the contribution of opioids, 5 mg/kg naloxone hydrochloride was injected intravenously (tail vein) 30 minutes before recordings, and mice received intradermal DCA at 0 and 180 minutes of recordings. To determine whether mast cells participate in BA-induced scratching, the mast cell stabilizer and H_1 receptor antagonist ketotifen (1 mg/kg i.p.) or vehicle (0.9% NaCl) was administered to mice 5 minutes before DCA injection. The role of TGR5 in LPA-evoked scratching was examined by comparing scratching in *Tgr5*-WT and *Tgr5*-KO mice after intradermal injection of LPA (100 μg). Scratching behavior was quantified by 2 observers unaware of test agents or genotypes. 1 scratch was defined as lifting the hind limb to the injection site and then a placing of the paw on the floor, regardless of the number of strokes. If counts differed by greater than 3 scratches over a 30-minute period, both observers reevaluated the record. Results were expressed as the number of scratching events during 15, 30, or 60 minutes of observation.

Pain behavior. *Tgr5*-WT, *Tgr5*-KO, and *Tgr5*-Tg mice were studied (male and female, 6–20 weeks of age). Mice were placed in individual cylinders on a mesh stand. Mice were acclimatized to the experimental room, restraint apparatus, and investigator for 2-hour periods on 2 successive days before experiments. To assess mechanical pain, paw withdrawal in response to stimulation of the plantar surface of the hind paw with graded von Frey filaments (0.078, 0.196, 0.392, 0.686, 1.569, 3.922, 5.882, 9.804, 13.725, and 19.608 mN) was determined using the "up-and-down" paradigm (68). In this analysis, an increase in the filament stiffness required to induce paw withdrawal indicates mechanical analgesia, whereas a decrease in the filament stiffness required to induce withdrawal indicates mechanical hyperalgesia. To assess inflammatory edema of the paw, hind paw thickness was measured using digital calipers before and after treatments. On the day before the study, von Frey scores were measured in triplicate to establish a baseline for each animal. For peripheral administration of test agents, mice were sedated with 5% isoflurane, and DCA, TLCA, OA, or UDCA (12.5–125 μg); capsaicin (5 μg); or vehicle (0.9% NaCl, 10 μl) was injected subcutaneously into the plantar surface of 1 hind paw. For central administration of test agents, DCA or UDCA (0.25–25 μg) or vehicle (0.9% NaCl, 5 μl) was injected intrathecally (L4/L5) in conscious mice. von Frey score and paw thickness were determined 60–240 minutes after injection. To evaluate the contribution of opioids released locally within the paw to analgesia induced by peripherally administered BA, naloxone hydrochloride (5 μg, 10 μl) or vehicle (0.9% NaCl, 10 μl) was administered by intraplantar injection 2 hours after intraplantar injection of DCA (25 μg). To assess the involvement of opioids to analgesia induced by central administration of BAs, naloxone hydrochloride (5 mg/kg) or vehicle (0.9% NaCl) was injected intravenously (tail vein) 2 hours after an intrathecal injection of DCA (25 μg). Investigators were unaware of test agents or genotypes. von Frey scores and paw thickness were expressed as percent of basal value.

TGR5 activation assay. HEK293 cells stably expressing human TGR5 were generated and maintained as described previously (39). TGR5 activation was assessed by measuring cAMP formation. Cells (10,000 cells per 5 μl) were suspended in phenol red–free DMEM containing 10% FBS, 0.1% BSA,

and 1 mM 3-isobutyl-1-methylxanthine and were stimulated with DCA or LPA (18:1; 10^{-12} M to 10^{-2} M) for 30 minutes at 37°C. Cells were lysed with 1 volume of 0.3% Tween 20, 5 mM HEPES, and 0.1% BSA in water (pH 7.4). cAMP in the lysate was assayed using ALPHA-screen, according to the manufacturer's instructions (PerkinElmer Life Sciences).

Statistics. Data are expressed as mean ± SEM. Data were compared statistically using Graphpad Prism 5. Differences between 2 groups were examined using paired 2-tailed *t* tests (excitability of the same neurons and neuropeptide release from the same tissues before and after BA exposure) or unpaired 2-tailed *t* tests (excitability of different neurons or behavioral responses of different mice treated with vehicle or test agents). Differences among multiple groups were examined using ANOVA and Student-Newman-Keuls post-hoc test (behavioral studies using multiple test agents or mouse genotypes) or Dunnett post-hoc test (excitability of different neurons incubated with graded concentrations of BAs). A *P* value less than 0.05 was considered significant.

Study approval. The Institutional Animal Care and Use Committees of Monash Institute of Pharmaceutical Sciences, UCSF, Queen's University, and University of Florence approved all studies on animals.

Acknowledgments

We thank Cody Godfrey, Jonathan Chiu, and Tao Yu for technical assistance. The authors were supported by NIH/NIDDK grants DK39957, DK43207, and DK57840, NHMRC grants 63303 and 103188, and Monash University (to N.W. Bunnett); by Northern California Institute for Research and Education, Veterans Health Administration, and NIH/NIDDK grant P30-DK026743 (to C.U. Corvera); by NIH/NIAMS grant 59402-01A1 (to M. Steinhoff); by NHMRC grant 454858 (to D.P. Poole); by Ecole Polytechnique Fédérale de Lausanne and Swiss National Science Foundation (SNF) grant 31003A_125487 (to K. Schoonjans); by British Heart Foundation grant FS/08/017/25027 (to G.S. Cottrell); and by Regione Toscana (FABER - POR CREO, FESR 2007-2013 1.1.C.) and the Italian Institute of Technology (Project SEED) (to P. Geppetti).

Received for publication April 30, 2012, and accepted in revised form January 17, 2013.

Address correspondence to: Nigel Bunnett, Monash Institute of Pharmaceutical Sciences, 381 Royal Parade, Parkville, Victoria 3052, Australia. Phone: 61.3.9903.9136; Fax: 61.3.9903.9581; E-mail: Nigel.Bunnett@Monash.edu. Or to: Carlos U. Corvera, Department of Surgery, University of California, San Francisco, VA Medical Center, Surgical Service, 4150 Clement Street, Suite 112, San Francisco, California 94121, USA. Phone: 415.221.4180, ext. 4019; Fax: 415.353.9931; E-mail: Carlos.corvera@ucsfmedctr.org.

1. European Association for the Study of the Liver. EASL Clinical Practice Guidelines: management of cholestatic liver diseases. *J Hepatol*. 2009;51(2):237–267.
2. Bergasa NV. The itch of liver disease. *Semin Cutan Med Surg*. 2011;30(2):93–98.
3. Fitzgerald JE, White MJ, Lobo DN. Courvoisier's gallbladder: law or sign? *World J Surg*. 2009;33(4):886–891.
4. Moretti EW, Robertson KM, Tuttle-Newhall JE, Clavien PA, Gan TJ. Orthotopic liver transplant patients require less postoperative morphine than do patients undergoing hepatic resection. *J Clin Anesth*. 2002;14(6):416–420.
5. Nelson L, Vergnolle N, D'Mello C, Chapman K, Le T, Swain MG. Endogenous opioid-mediated antinociception in cholestatic mice is peripherally, not centrally, mediated. *J Hepatol*. 2006;44(6):1141–1149.
6. Patel KN, Dong X. An itch to be scratched. *Neuron*. 2010;68(3):334–339.
7. Ward L, Wright E, McMahon SB. A comparison of the effects of noxious and innocuous counterstimuli on experimentally induced itch and pain. *Pain*. 1996;64(1):129–138.
8. Slappendel R, Weber EW, Benraad B, van Limbeek J, Dirksen R. Itching after intrathecal morphine. Incidence and treatment. *Eur J Anaesthesiol*. 2000;17(10):616–621.
9. Schmelz M, Schmidt R, Bickel A, Handwerker HO, Torebjork HE. Specific C-receptors for itch in human skin. *J Neurosci*. 1997;17(20):8003–8008.
10. Sun YG, Chen ZF. A gastrin-releasing peptide receptor mediates the itch sensation in the spinal cord. *Nature*. 2007;448(7154):700–703.
11. Sun YG, Zhao ZQ, Meng XL, Yin J, Liu XY, Chen ZF. Cellular basis of itch sensation. *Science*. 2009; 325(5947):1531–1534.
12. Liu XY, et al. Unidirectional cross-activation of GRPR by MOR1D uncouples itch and analgesia induced by opioids. *Cell*. 2011;147(2):447–458.
13. Schmelz M, Schmidt R, Weidner C, Hilliges M, Torebjork HE, Handwerker HO. Chemical response pattern of different classes of C-nociceptors to pruritogens and algogens. *J Neurophysiol*. 2003; 89(5):2441–2448.
14. Imamachi N, et al. TRPV1-expressing primary afferents generate behavioral responses to pruritogens via multiple mechanisms. *Proc Nat Acad Sci*. 2009;106(27):11330–11335.
15. Lagerstrom MC, et al. VGLUT2-dependent sensory neurons in the TRPV1 population regulate pain and itch. *Neuron*. 2010;68(3):529–542.
16. Liu Y, et al. VGLUT2-dependent glutamate release from nociceptors is required to sense pain and suppress itch. *Neuron*. 2010;68(3):543–556.
17. McMahon SB, Koltzenburg M. Itching for an explanation. *Trends Neurosci*. 1992;15(12):497–501.
18. Magyar I, Loi HG, Feher T. Plasma bile acid levels and liver disease. *Acta Med Acad Sci Hung*. 1981; 38(2):109–115.
19. Schoenfield LJ, Sjorvall J, Perman E. Bile acids on the skin of patients with pruritic hepatobiliary disease. *Nature*. 1967;213:93–94.
20. Kirby J, Heaton KW, Burton JL. Pruritic effect of bile salts. *Br Med J*. 1974;4(5946):693–695.
21. Varadi DP. Pruritus induced by crude bile and purified bile acids. Experimental production of pruritus in human skin. *Arch Dermatol*. 1974;109(5):678–681.
22. Mela M, Mancuso A, Burroughs AK. Review article: pruritus in cholestatic and other liver diseases. *Aliment Pharmacol Ther*. 2003;17(7):857–870.
23. Thornton JR, Losowsky MS. Plasma leucine enkephalin is increased in liver disease. *Gut*. 1989; 30(10):1392–1395.
24. Swain MG, Rothman RB, Xu H, Vergalla J, Bergasa NV, Jones EA. Endogenous opioids accumulate in plasma in a rat model of acute cholestasis. *Gastroenterology*. 1992;103(2):630–635.
25. Bergasa NV, Rothman RB, Vergalla J, Xu H, Swain MG, Jones EA. Central mu-opioid receptors are down-regulated in a rat model of cholestasis. *J Hepatol*. 1992;15(1–2):220–224.
26. Bergasa NV, et al. A controlled trial of naloxone infusions for the pruritus of chronic cholestasis. *Gastroenterology*. 1992;102(2):544–549.
27. Thomas C, Pellicciari R, Pruzanski M, Auwerx J, Schoonjans K. Targeting bile-acid signalling for metabolic diseases. *Nat Rev Drug Discov*. 2008; 7(8):678–693.
28. Kawamata Y, et al. A G protein-coupled receptor responsive to bile acids. *J Biol Chem*. 2003; 278(11):9435–9440.
29. Maruyama T, et al. Identification of membrane-type receptor for bile acids (M-BAR). *Biochem Biophys Res Commun*. 2002;298(5):714–719.
30. Watanabe M, et al. Bile acids induce energy expenditure by promoting intracellular thyroid hormone activation. *Nature*. 2006;439(7075):484–489.
31. Katsuma S, Hirasawa A, Tsujimoto G. Bile acids promote glucagon-like peptide-1 secretion through TGR5 in a murine enteroendocrine cell line STC-1. *Biochem Biophys Res Commun*. 2005;329(1):386–390.
32. Thomas C, et al. TGR5-mediated bile acid sensing controls glucose homeostasis. *Cell Metab*. 2009; 10(3):167–177.
33. Keitel V, Cupisti K, Ullmer C, Knoefel WT, Kubitz R, Haussinger D. The membrane-bound bile acid receptor TGR5 is localized in the epithelium of human gallbladders. *Hepatology*. 2009;50(3):861–870.
34. Lavoie B, et al. Hydrophobic bile salts inhibit gallbladder smooth muscle function via stimulation of GPBAR1 receptors and activation of KATP channels. *J Physiol*. 2010;588(pt 17):3295–3305.
35. Li T, et al. The G protein-coupled bile acid receptor, TGR5, stimulates gallbladder filling. *Mol Endocrinol*. 2011;25(6):1066–1071.
36. Maruyama T, et al. Targeted disruption of G protein-coupled bile acid receptor 1 (Gpbar1/M-Bar) in mice. *J Endocrinol*. 2006;191(1):197–205.
37. Pols TW, et al. TGR5 Activation Inhibits Atherosclerosis by Reducing Macrophage Inflammation and Lipid Loading. *Cell Metab*. 2011;14(6):747–757.
38. Wang YD, Chen WD, Yu D, Forman BM, Huang W. The G-Protein-coupled bile acid receptor, Gpbar1 (TGR5), negatively regulates hepatic inflammatory response through antagonizing nuclear factor kappa light-chain enhancer of activated B cells (NF-kappaB) in mice. *Hepatology*. 2011;54(4):1421–1432.
39. Poole DP, et al. Expression and function of the bile acid receptor GpBAR1 (TGR5) in the murine enteric nervous system. *Neurogastroenterol Motil*. 2010;22(7):814–825, e227–818.
40. Keitel V, et al. The bile acid receptor TGR5 (Gpbar-1) acts as a neurosteroid receptor in brain. *Glia*. 2010;58(15):1794–1805.
41. Sato H, et al. Novel potent and selective bile acid derivatives as TGR5 agonists: biological screening, structure-activity relationships, and molecular modeling studies. *J Med Chem*. 2008;51(6):1831–1841.
42. Liu T, et al. TLR3 deficiency impairs spinal cord synaptic transmission, central sensitization, and pruritus in mice. *J Clin Invest*. 2012;122(6):2195–2207.
43. Shim WS, et al. TRPV1 mediates histamine-induced

itching via the activation of phospholipase A2 and 12-lipoxygenase. *J Neurosci*. 2007;27(9):2331–2337.
44. Wilson SR, et al. TRPA1 is required for histamine-independent, Mas-related G protein-coupled receptor-mediated itch. *Nat Neurosci*. 2011;14(5):595–602.
45. Bunnett NW, et al. Canine bombesin-like gastrin releasing peptides stimulate gastrin release and acid secretion in the dog. *J Physiol*. 1985;365:121–130.
46. Labuz D, et al. Peripheral antinociceptive effects of exogenous and immune cell-derived endomorphins in prolonged inflammatory pain. *J Neurosci*. 2006;26(16):4350–4358.
47. Kayssi A, Amadesi S, Bautista F, Bunnett NW, Vanner S. Mechanisms of protease-activated receptor 2-evoked hyperexcitability of nociceptive neurons innervating the mouse colon. *J Physiol*. 2007; 580(pt 3):977–991.
48. Sato H, et al. Anti-hyperglycemic activity of a TGR5 agonist isolated from Olea europaea. *Biochem Biophys Res Commun*. 2007;362(4):793–798.
49. Iguchi Y, Nishimaki-Mogami T, Yamaguchi M, Teraoka F, Kaneko T, Une M. Effects of chemical modification of ursodeoxycholic acid on TGR5 activation. *Biol Pharm Bull*. 2011;34(1):1–7.
50. Fleming MS, Ramos D, Han SB, Zhao J, Son YJ, Luo W. The majority of dorsal spinal cord gastrin releasing peptide is synthesized locally whereas neuromedin B is highly expressed in pain- and itch-sensing somatosensory neurons. *Mol Pain*. 2012;8(1):52.
51. Glazer EJ, Basbaum AI. Immunohistochemical localization of leucine-enkephalin in the spinal cord of the cat: enkephalin-containing marginal neurons and pain modulation. *J Comp Neurol*. 1981; 196(3):377–389.
52. Weidner C, et al. Acute effects of substance P and calcitonin gene-related peptide in human skin—a microdialysis study. *J Invest Dermatol*. 2000; 115(6):1015–1020.
53. Heinz-Erian P, Coy DH, Tamura M, Jones SW, Gardner JD, Jensen RT. [D-Phe12]bombesin analogues: a new class of bombesin receptor antagonists. *Am J Physiol*. 1987;252(3 pt 1):G439–G442.
54. Ko MC, Naughton NN. An experimental itch model in monkeys: characterization of intrathecal morphine-induced scratching and antinociception. *Anesthesiology*. 2000;92(3):795–805.
55. Hashimoto T, Ohata H, Momose K. Itch-scratch responses induced by lysophosphatidic acid in mice. *Pharmacol*. 2004;72(1):51–56.
56. Kremer AE, et al. Lysophosphatidic acid is a potential mediator of cholestatic pruritus. *Gastroenterology*. 2010;139(3):1008–1018.
57. Koga K, et al. Glutamate acts as a neurotransmitter for gastrin releasing peptide-sensitive and insensitive itch-related synaptic transmission in mammalian spinal cord. *Mol Pain*. 2011;7:47.
58. Angelin B, Bjorkhem I, Einarsson K, Ewerth S. Hepatic uptake of bile acids in man. Fasting and postprandial concentrations of individual bile acids in portal venous and systemic blood serum. *J Clin Invest*. 1982;70(4):724–731.
59. Mano N, et al. Presence of protein-bound unconjugated bile acids in the cytoplasmic fraction of rat brain. *J Lipid Res*. 2004;45(2):295–300.
60. Ogundare M, et al. Cerebrospinal fluid steroidomics: are bioactive bile acids present in brain? *J Biol Chem*. 2010;285(7):4666–4679.
61. Bron B, Waldram R, Silk DB, Williams R. Serum, cerebrospinal fluid, and brain levels of bile acids in patients with fulminant hepatic failure. *Gut*. 1977;18(9):692–696.
62. Bartholomew TC, Summerfield JA, Billing BH, Lawson AM, Setchell KD. Bile acid profiles of human serum and skin interstitial fluid and their relationship to pruritus studied by gas chromatography-mass spectrometry. *Clin Sci*. 1982;63(1):65–73.
63. Lieu T, Undem BJ. Neuroplasticity in vagal afferent neurons involved in cough. *Pul Pharm Ther*. 2011;24(3):276–279.
64. Gibbins IL, Furness JB, Costa M, MacIntyre I, Hillyard CJ, Girgis S. Co-localization of calcitonin gene-related peptide-like immunoreactivity with substance P in cutaneous, vascular and visceral sensory neurons of guinea pigs. *Neurosci Lett*. 1985; 57(2):125–130.
65. Cuello AC, Galfre G, Milstein C. Detection of substance P in the central nervous system by a monoclonal antibody. *Proc Nat Acad Sci*. 1979;76(7):3532–3536.
66. Lucchinetti CF, Kimmel DW, Lennon VA. Paraneoplastic and oncologic profiles of patients seropositive for type 1 antineuronal nuclear autoantibodies. *Neurol*. 1998;50(3):652–657.
67. Amadesi S, et al. Protease-activated receptor 2 sensitizes the capsaicin receptor transient receptor potential vanilloid receptor 1 to induce hyperalgesia. *J Neurosci*.2004;24(18):4300–4312.
68. Chaplan SR, Bach FW, Pogrel JW, Chung JM, Yaksh TL. Quantitative assessment of tactile allodynia in the rat paw. *J Neurosci Meth*. 1994;53(1):55–63.